Hyperparameter Tuning for Causal Inference with Double Machine Learning: A Simulation Study

Author names withheld

Editor: Under Review for CLeaR 2024

Abstract

Proper hyperparameter tuning is essential for achieving optimal performance of modern machine learning (ML) methods in predictive tasks. While there is an extensive literature on tuning ML learners for prediction, there is only little guidance available on tuning ML learners for causal machine learning and how to select among different ML learners. In this paper, we empirically assess the relationship between the predictive performance of ML methods and the resulting causal estimation based on the Double Machine Learning (DML) approach by Chernozhukov et al. (2018). DML relies on estimating so-called nuisance parameters by treating them as supervised learning problems and using them as plug-in estimates to solve for the (causal) parameter. We conduct an extensive simulation study using data from the 2019 Atlantic Causal Inference Conference Data Challenge. We provide empirical insights on the role of hyperparameter tuning and other practical decisions for causal estimation with DML. First, we assess the importance of data splitting schemes for tuning ML learners within Double Machine Learning. Second, we investigate how the choice of ML methods and hyperparameters, including recent AutoML frameworks, impacts the estimation performance for a causal parameter of interest. Third, we assess to what extent the choice of a particular causal model, as characterized by incorporated parametric assumptions, can be based on predictive performance metrics.

Keywords: Causal Machine Learning, Hyperparameter Tuning, Causal Inference, Double Machine Learning

1. Introduction

Double/Debiased machine learning (DML) is an estimation framework for causal parameters as based on ML-estimated nuisance functions that has been established by Chernozhukov et al. (2018). DML combines the strengths of machine learning for prediction with estimation and inference of causal parameters. The major idea of the double machine learning framework is to make the estimation framework robust to inherent biases of ML estimation: To address the bias-variance tradeoff, ML methods introduce some regularization. Without any further adaption of the estimation procedure this will effectively translate into a bias of the causal parameter of interest. To overcome these shortcomings, the double machine learning approach combines three key ingredients (Bach et al., 2022, 2021): (i) Identification of causal parameters through Neyman-orthogonal moment conditions, (ii) high-quality machine learning estimators and (iii) sample splitting. Incorporating these ingredients makes it possible to establish $\sqrt{N}$ convergence and asymptotic normality of the causal estimator. In recent years, the DML framework has become popular in various disciplines, including econometrics (Knaus, 2022), reinforcement learning (Narita et al., 2020) and management science (Schacht et al., 2023). Whereas there is an extensive literature and ample benchmark studies on hyperparameter tuning approaches in predictive ML tasks, for example see Bischl et al. (2021), there is a considerable gap on the interaction between the predictive performance and the quality

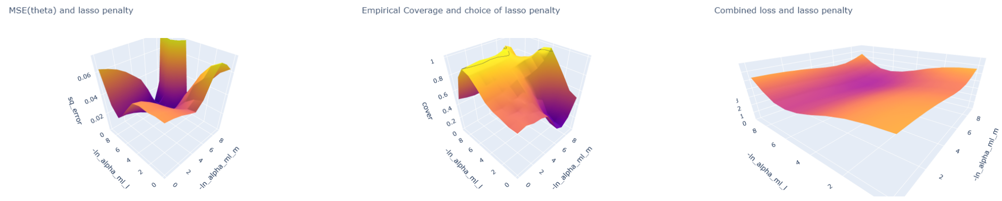

(a) (b) (c)

Figure 1: Average results from 100 repetitions for a simulated data example, BCH DGP with $n = 100$ observations and $p = 200$ explanatory variables. The figures show various metrics as obtained for lasso penalty for the nuisance components $\eta_0 = (\ell_0, m_0)$. Panel (a): Mean squared error, Panel (b): Empirical coverage of true parameter, Panel (c): Combined loss for PLR.

in terms of causal estimation. Several studies investigate model selection strategies for different estimation approaches that are based on ML, mostly with a focus on heterogeneous treatment effects (Schuler et al., 2018; Mahajan et al., 2022). Previous studies with a specific focus on DML compare different sample splitting schemes (Okasa, 2022) or different ML learners (Knaus et al., 2020) for estimation of heterogeneous treatment effects based on synthetic or semi-synthetic data. However, the question of how to select learners within the DML framework remains unclear in the existing literature. Few studies address the aspect of hyperparameter tuning in the context of double machine learning. The approach by Fingerhut et al. (2022) is based on a target metric that combines the predictive losses from two predictive tasks incorporated in partially linear regression models. Chernozhukov et al. (2022) provide a multitask framework for neural networks that is based on a general Riesz representation. In this work, we will perform a thorough empirical study to show that hyperparameter tuning is required when using DML in order to achieve optimal inference on the target parameter. We assess different data splitting schemes for the tuning process, draw connections between the predictive performance of the ML learners and the error of the causal estimate and give recommendations on the selection of the causal model.

2. Problem Setting: Learners, Hyperparameters and Sample Splitting

2.1. The role of learners in double machine learning

In DML, the goal is estimation and inference on a target parameter θ_0 in the presence of a high-dimensional nuisance parameter. Importantly, identification in DML is based on an orthogonal moment condition with a score function $\psi(W;\theta,\eta)$, namely

$$E[\psi(W;\theta_0,\eta_0] = 0,$$

with data W, true value of the causal parameter θ_0 is and nuisance function η_0. The general idea is to use ML methods to estimate each of the nuisance parameters, plug them into the score function and solve for the target parameter. A key condition for valid inference is so-called Neyman-orthogonality

$$\partial_\eta \mathbb{E}[\psi(W;\theta_0,\eta)]|_{\eta=\eta_0} = 0.$$

∂_η denotes the pathwise Gateaux derivative operator. Neyman-orthogonality ensures that the moment condition identifying θ_0 is insensitive to small perturbations of the nuisance function η around η_0 under relatively general assumptions. This eliminates the first-order bias which might stem from regularization, when replacing η_0 by the ML estimate $\hat{\eta}_0$. Formally, the learner requirement applies to the rates of convergence of the employed ML prediction methods. If the used ML estimators do converge sufficiently fast, the bias in $\hat{\eta}_0$ will eventually vanish in the limit, giving rise to a $\sqrt{N}$-consistent and normally distributed estimate $\hat{\theta}_0$. The theoretical framework of Chernozhukov et al. (2018) specifies structural assumptions that guides the choice of the ML learners. For example, under the assumption of sparsity, ℓ_1 penalized estimators such as the lasso (Tibshirani, 1996) are known to satisfy the rate criterion for estimating η_0, such that it can be used for causal estimation of θ_0. Generally, the theoretical criterion on the learners refers to the error in the composed nuisance term η_0, which collects multiple prediction problems in a so-called *combined loss*, which is specific to a particular causal model and orthogonal score formulation (Chernozhukov et al., 2018). How to select among different ML learners for the nuisance part, is key for practical applications and understanding this better has been a main motivation for this study.

To make the role of the learners in DML more tractable, we will briefly introduce two causal models that will also be used in our simulation study: The Partially Linear Regression (PLR) model and the Interactive Regression Model (IRM). Under common assumptions for identification such as unconfoundedness, the PLR can be used to estimate the Average Treatment Effect (ATE) of a binary or continuous treatment variable D on an outcome Y. The PLR incorporates a partially linear additive structure, i.e., the causal effect is constant for all individuals

$$\begin{aligned} Y &= D\theta_0 + g_0(X) + \xi, \quad \mathbb{E}[\xi \mid X, D] = 0 \\ D &= m_0(X) + V, \quad \mathbb{E}[V \mid X] = 0 \end{aligned}$$

Using the so-called partialling out score, the corresponding nuisance component comprises two functions, $\eta_0 = (\ell_0, m_0) = (\mathbb{E}[Y|X], \mathbb{E}[D|X])$. The IRM imposes weaker functional form assumptions and makes it possible to estimate heterogeneous treatment effects. Thus, the nuisance component g_0 can also model interactions between D and Y.

$$\begin{aligned} Y &= g_0(D, X) + \xi, \quad \mathbb{E}[\xi \mid X, D] = 0 \\ D &= m_0(X) + V, \quad \mathbb{E}[V \mid X] = 0 \end{aligned}$$

Using the doubly robust score which identifies the ATE of a binary treatment variable D on Y, the nuisance parameter comprises two functions $\hat{\eta}_0 = (g_0, m_0) = (\mathbb{E}[Y|D, X], \mathbb{E}[D|X])$. Double machine learning is closely related to “double robustness” and DML-based estimators build on doubly robust scores (Robins et al. (1994)) and their augmented inverse probability weighting estimators. Doubly robust estimators, which rely on two nuisance parameters (outcome regression and propensity score), are robust against misspecification of one of the nuisance parameters. Hence, whenever it is possible to estimate one nuisance component at the parametric rate, DR estimators tolerate slower rates for the other nuisance component. DML generalizes this idea to a broader class of causal models and formulates the rate requirement in terms of a model-specific *combined loss*. For the PLR and IRM, their definition is provided in Table 4. For a detailed discussion we refer to Knaus (2022) and Smucler et al. (2019). Finally, we would like to note that DML is also closely related to target maximum likelihood learning (van der Laan and Rubin (2006)).

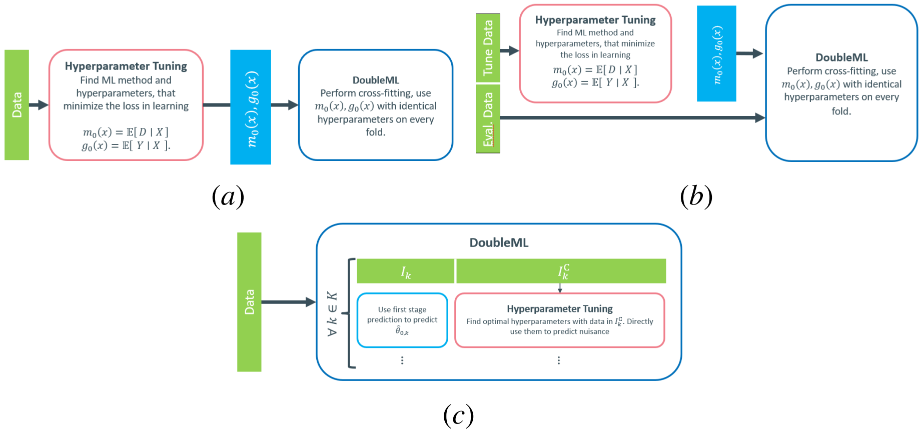
Data
Hyperparameter Tuning
Find ML method and hyperparameters, that minimize the loss in learning
$m_0(x) = \mathbb{E}[D \mid X]$
$g_0(x) = \mathbb{E}[Y \mid X]$.
$m_0(x), g_0(x)$
DoubleML
Perform cross-fitting, use $m_0(x), g_0(x)$ with identical hyperparameters on every fold.
(a)
Tune Data
Eval. Data
Hyperparameter Tuning
Find ML method and hyperparameters, that minimize the loss in learning
$m_0(x) = \mathbb{E}[D \mid X]$
$g_0(x) = \mathbb{E}[Y \mid X]$.
$m_0(x), g_0(x)$
DoubleML
Perform cross-fitting, use $m_0(x), g_0(x)$ with identical hyperparameters on every fold.
(b)
Data
DoubleML
$\forall k \in K$
I_k
I_k^C
Use first stage prediction to predict $\hat{\theta}_{0,k}$
Hyperparameter Tuning
Find optimal hyperparameters with data in I_k^C. Directly use them to predict nuisance
(c)

Figure 2: Schematic representation of sample splitting approaches for hyperparameter tuning: Panel (a) *full sample*, (b) *split sample*, (c) *on folds*.

2.2. Choice of hyperparameters in double machine learning

Figure 1 serves as a simplified illustration of the role of an appropriate hyperparameter choice for the causal estimation quality. It shows the mean squared error with respect to the true causal parameter θ_0 in Panel (a), the empirical coverage in Panel (b) and the combined loss in the PLR in Panel (c) as obtained for a grid of lasso-penalty values. The example is based on a high-dimensional sparse data generating process with $n = 100$ observations and $p = 200$ explanatory variables as presented in Belloni et al. (2013), which we refer to as BCH. In a PLR model, the lasso can be used as an appropriate learner for the sparse nuisance relationships $\eta_0 = (\ell_0, m_0)$. The surface plots illustrate that an appropriate choice of the hyperparameter, i.e., the lasso penalty λ, is essential for a precise estimator of θ_0. The figures show that it is important to have suitable estimation performance in both nuisance components ℓ_0 and m_0 in order to obtain a low mean squared error for the causal parameter as well as to achieve the nominal coverage of the confidence intervals. In line with the theoretical foundation of the DML approach, Panel (c) of Figure 1 reveals that a lower combined loss for the nuisance component corresponds to a better estimation performance and higher coverage in Panel (a) and (b). An additional motivating example that highlights the importance of an appropriate hyperparameter choice in terms of the empirical distribution of the DML estimator is provided in Appendix A.

2.3. Cross-fitting and forms of data splitting

In addition to using an orthogonal score function for identification and appropriate ML estimation of the nuisance part, DML incorporates sample-splitting as a third ingredient. Splitting the sample in different partitions makes it possible to abstract from (small) overfitting biases. Sample splitting guarantees the independence of the samples that are (i) used to learn the nuisance functions η_0 (training data) and (ii) used to solve the orthogonal score with regard to the causal parameter θ_0 (holdout data). Cross-fitting is an efficient form of data splitting, that uses all the available data by swapping the roles of the training and holdout data in a cross-validated manner. Cross-fitting proceeds as (Chernozhukov et al., 2018): (1) Take a K-fold random partition $(I_k)_{k=1}^K$ of

Learner	Implementation	Tuning Procedure and Parameters	Fixed Parameters
Lasso	`Scikit-learn` (Pedregosa et al., 2011)	Internal cross-validated fitting of ℓ_1 regularization parameter	5-fold CV
Random Forest	`Scikit-learn` (Pedregosa et al., 2011)	Cross-validated grid search for tree depth (4,5,6).	100 trees[1], 5-fold CV
Extreme Gradient Boosting	`xgboost` (Chen and Guestrin, 2016)	Cross-validated grid search for number of trees (up to 100 with early stopping)	Tree-depth 2, learning rate 0.1, 5-fold CV
AutoML	`FLAML` (Wang and Wu, 2019)	Computation time of 60s[2]	

Table 1: Overview of the learners and tuning grids used in the simulation study.

observation indices $\{1, \dots, N\}$ such that the size of each fold I_k is $n = N/K$. For each $\{1, \dots, K\}$, define $I_k^{\mathsf{C}} := \{1, \dots, N\} \setminus I_k$. (2) For each $k \in K$, construct an ML estimator $\hat{\eta}_{0,k}$ based on the observations $i \in I_k^{\mathsf{C}}$. (3) For each $k \in K$, construct the estimator $\hat{\theta}_0$ using the empirical expectation of the estimator using the observations $i \in I_k$ and average over the K folds. This procedure refers to fitting the nuisance learners and does not explicitly address hyperparameter tuning and similar considerations. Sample splitting and resampling is crucial to avoid overfitting in predictive machine learning (Bischl et al., 2023). There are different ways to combine the DML cross-fitting procedure with ML tuning cross-validation schemes in practice. In our simulation study, we investigate three sample splitting approaches when tuning the nuisance estimators, which are illustrated in Figure 2. **Full sample**: We apply cross-validated tuning on the whole sample and find the best learner and the best hyperparameter configuration by minimizing a loss target for each of the nuisance prediction tasks. Causal estimation by DML is also performed on all observations according to the cross-fitting algorithm, using the same learner and set of hyperparameters on all folds. The splits in the cross-validation scheme for tuning and the splits in the DML cross-fitting algorithms are independent of each other. **Split sample**: Splitting the data into a tuning and an inference fold is frequently employed in predictive machine learning. We adapt it by splitting the sample in half and tune the hyperparameters using cross-validation on 50% of the data only. We choose the optimal learner and hyperparameter set and use them for fitting the nuisance functions in the remaining 50% observations using DML cross-fitting. In this schedule, the samples used for tuning and causal estimation do not overlap. Hence, fitting the ML learners only uses data that has not been used for tuning. **On folds**: We perform sample splitting as in the cross-fitting algorithm and perform cross-validated hyperparameter tuning within each of the cross-fitting folds: We take a K-fold random partition $(I_k)_{k=1}^K$ of observation indices $[N] = \{1, \dots, N\}$ such that the size of each fold I_k is $n = N/K$. For each $k \in [K]$, we perform cross-validation based hyperparameter optimization with the observations $i \notin I_k$ directly on the same partition (or fold) which is used for predicting the nuisance components. This approach takes K-times the calculation power of the other two. With our empirical results, we would like to investigate how the cross-fitting scheme of DML and the cross-validation splitting schemes for hyperparameter tuning interact, for example, comparing the split sample approach with non-overlapping subsamples to the overlapping, but independent sample splits of the full sample and on folds approach.

3. Set-up of the Simulation Study

The empirical assessment of causal estimators is generally limited by the fact that the ground truth (i.e., the true value of the causal parameter θ_0) is not observable in real data sets. Hence, empirical studies have to rely on simulated data sets. To investigate the role of different sample splitting schemes, the choice of learners and hyperparameters as well as the scope to which predictive metrics can be used to motivate the choice of a causal model (PLR vs. IRM), we use two sources of data. Our major analysis

DGP	D on Y	X on D	X on Y	ε	θ	oracle bias (%)	oracle std	SNR	n
1	linear, additive	linear	linear	$N(0,2)$	0.2	7.4472	0.1318	0.404	1000
2	linear, additive	non-linear	non-linear	$N(0,1)$	0.8	0.0289	0.0703	0.462	1000
3	linear, additive	linear, sparse	linear, sparse	$N(0,1)$	-0.8	0.0039	0.0738	0.985	1000
4	linear, additive	non-linear	non-linear	$t(5)$	2.1	0.4789	0.0541	0.842	2000
5	interacts with 11 X_i and ε	non-linear	non-linear	$t(12)$	-0.3429	2.2763	0.0861		2000
6	interacts with 1 X_i and ε	linear	linear	$t(19)$	-1.1039	0.0021	0.0718		1000
7	No effect	non-linear	non-linear	$N(0,1)$	0		0.0511	0.905	2000
8	interacts with 5 X_i	non-linear	non-linear	$N(0,0.02)$	-1.432	0.0065	0.0143	12.463	1000
9	interacts with 2 X_i	non-linear	non-linear	$N(0,3)$	12.62	-0.0181	0.0952	12.284	2000
10	interacts with 3 X_i	non-linear	linear	$t(4)$	9.134	0.0057	0.1206	11.676	2000
11	interacts with 23 X_i	linear	non-linear	$N(0,2)$	10.77	0.0338	0.0547	61.092	2000
12	interacts with 7 X_i	non-linear	non-linear	$N(0,2)$	-3.159	-0.0011	0.1009	12.820	2000
13	interacts with 1 X_i	non-linear	non-linear	dependent on D	-0.8486	0.0871	0.0402		2000
14	interacts with 4 X_i	non-linear	non-linear	$N(0,4)$	61.11	-0.0074	1.2539	219.221	1000
15	interacts with 2 X_i	non-linear	non-linear	dependent on D	-0.1606	-0.3792	0.0254		2000
16	linear, additive	linear	linear	$t(8)$	1	-0.0316	0.0553	10.934	2000

Table 2: Details on the data generating processes, with description of relationships and error term, true parameter, oracle estimate and standard error, sample size and signal to noise ratio (SNR). The SNR is calculated empirically from the DGPs, by calculating $Var(Y)/Var(\varepsilon)$ for each repetition and averaging. Full description of the DGPs can be found in Appendix F.

will be based on data originally introduced for the 2019 Atlantic Causal Inference Conference (ACIC) data challenge[3]. We choose this data source because it generates designs with common and relatively complex empirical patterns under unconfoundedness.[4] Moreover, we focused on an external resource for the DGP as this helps to abstract from biases that might stem from using self-defined simulation scenarios. To gain more detailed insights, we used the BCH DGP by Belloni et al. (2013) as a second source. The advantage of this design is its clear structure, which makes it possible to match the empirical results with general theoretical reasoning. The ACIC data consist of 1600 data sets from 16 data generating processes with $n = 1000$ or $n = 2000$ observations and $p = 200$ covariates, a binary treatment variable and a continuous outcome. Table 2 contains a brief overview of the processes. A more detailed description can be found in Appendix F. The data generating processes are mostly in line with the unconfoundedness or conditional exogeneity assumption, $Y(d) \perp D \mid X$, with $Y(d)$ indicating the potential outcome under treatment $D = d$. Hence, these settings allow for identification of the average treatment effect, $\theta_0 = \mathbb{E}[Y(d = 1) - Y(d = 0)]$. Overall, the summary in Table 2 makes clear that the data generating processes of the ACIC challenge are very disparate, including settings with homogeneous and heterogeneous treatment effects, sparse and non-sparse, linear and non-linear settings, different values for the signal-to-noise ratio and varying values for the ATE across settings. In DGP 5 and 6, the unconfoundedness assumption is violated, which complicates estimation of the ATE. The information on the effect of D on Y is informative for the assumptions in the causal models introduced in Section 2. In cases of a linear and additive treatment effect of D on Y, the assumptions of the PLR are satisfied, such that it should allow for consistent estimation of θ_0. In case of interactions of D with other covariates, X, the functional form assumption of the PLR is violated, such that the resulting estimator is likely to be affected by a

[3] For more info, see https://sites.google.com/view/acic2019datachallenge/data-challenge.

[4] There are some scenarios, for which the unconfoundedness assumption will not hold exactly, see Table 2.

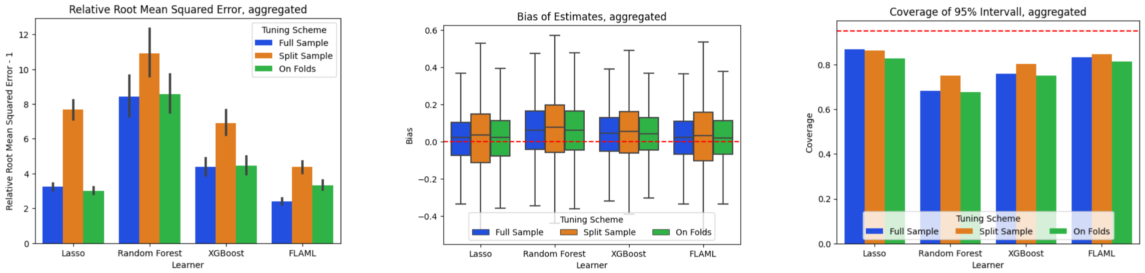

(*a*) (*b*) (*c*)

Figure 3: Average results on the ATE estimation over all ACIC DGPs, grouped by learner and sampling scheme. The groups show the learner, the colors the tuning scheme. The results refer to the causal model that is suitable for the underlying assumptions of the DGP, see Table 2. (a) Root mean squared error on the ATE parameter, relative to oracle and subtracted by -1. (b) Boxplot of bias on ATE parameter. (c) Coverage of the estimated 95% confidence interval with the true ATE parameter.

misspecification bias. The IRM, however, is more general, such that it should basically be suitable for causal estimation of θ_0 in both cases. As the PLR incorporates more structure, it is expected to lead to more efficient estimation in cases the underlying assumptions hold in the data generating process.

We study hyperparameter optimization with four different learners, including lasso, random forest (Breiman, 2001), extreme gradient boosting (Chen and Guestrin, 2016) and the AutoML learning framework FLAML (Wang and Wu, 2019). We focus on these learners as they are widely used in empirical research and industry practice. Moreover, the learners differ substantially in terms of the modeling assumptions and the way they introduce regularization to avoid overfitting. For example, the linear lasso learner uses an explicit penalty, whereas the nonlinear random forests and gradient boosting learners are based on ensembles of regression trees. As a result, these learners have different hyperparameters, which in turn affect the estimation performance in a different way (Probst et al., 2019). For random forests and gradient boosting, the hyperparameter choice is based on cross-validated search over a grid of values presented in Table 1. We use cross-validated lasso with the built-in penalty selection and the automated search for FLAML with a time budget of 60 seconds. As a tuning-free, but linear and low-dimensional benchmark, we compare our results to causal models that are based on linear and logistic regression.

4. Results

In this section we present results on different aggregation levels. Table 4 in Appendix C presents an overview on the different metrics.

4.1. Sample Splitting: Tuning and Causal Estimation

Tuning on the full sample or on folds exhibit similar performance, which is superior to the split sample approach in small samples. The first set of our results refer to the role of the sample splitting scheme that is used for hyperparameter optimization as described in Section 2.3. Figure 3

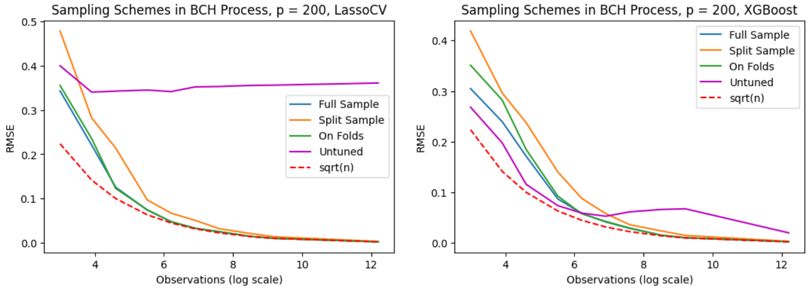

(a) (b)

Figure 4: Comparison of the RMSE on the ATE parameter of different sample splitting strategies in the BCH data generating process for (a) Lasso and (b) Boosting. Number of covariates in DGP is fixed, but n is increasing.

provides a summary of our results across all ACIC DGPs as obtained from 100 repetitions of every DGP. It presents an evaluation of the performance for different learners and sampling schemes based on a selection of the causal model (PLR, IRM) according to the underlying assumptions of the DGPs presented in Table 2.[5] [6] Panel (a) in Figure 3 shows the average root mean squared error relative to an oracle estimator for each of the employed learners and each sampling scheme as averaged over all DGPs. Panel (b) shows a boxplot of the bias of the corresponding causal estimates and the empirical coverage of 95% confidence intervals is depicted in Panel (c). The results reflect the main empirical finding that the *full sample* and *on folds* scheme perform similarly well. The only exception from this is the result on the AutoML learner, for which the adjusted tuning time for the on-folds scheme might not have been sufficient. The causal estimates obtained from the *split sample* approach are on average less accurate (in terms of the RMSE relative to an oracle) and more variable (cf. the boxplots in Panel (b)). This observation holds for virtually all learners and simulation settings considered as can be recognized from the Figures in E.1 and E.2 as well. We interpret these results as evidence of a considerable efficiency loss in finite samples by using only 50% of the observations for hyperparameter tuning. The empirical coverage of the confidence intervals are below the nominal level, which mainly reflects the differences in the underlying simulation settings. Due to the different structural assumptions across DGPs, it is unlikely that one learner will perform well in all settings.

The efficiency loss of the split sample approach vanishes with increasing sample size. We investigate to what extent the efficiency loss of the *split sample* approach persists with increasing samples size in Figure 4, which is based on data from the BCH DGP with $p = 200$ explanatory variables. In line with our previously reported results, the split sample scheme provides a higher RMSE on the causal parameter than the other two options. However, with growing number of observations, we observe that the RMSE of all tuning approaches converge with $\sqrt{n}$-rate. Thus, the difference between the schemes diminishes for larger samples.

[5] If θ_0 is additively separable, i.e., constant for all individuals, we use the PLR and the IRM otherwise. We select the results according to the causal model in order to abstract from model misspecification considerations.

[6] Due to the considerable differences in the simulation designs, we would like to note that Figure 3 is not entirely able to present a comprehensive picture of our extensive simulation results. We would like to refer readers to the more detailed results for every learner, sample splitting scheme and each causal model for each DGP in Appendix E.1 and E.2.

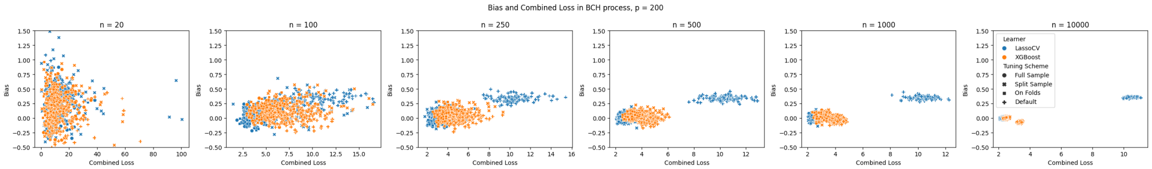

Figure 5: Combined Nuisance loss and bias in the BCH DGP with increasing sample size n for $p = 200$ explanatory variables. For large n/p, the tuned learner becomes more distinct in terms of both bias and combined nuisance loss.

4.2. Selection of Learners

The performance of the causal estimation depends on structural assumptions and appropriate learner choice. Comparing the four learners in the study, overall we find that the tuned AutoML and lasso learners perform very well across multiple settings (see Appendix E.1 and E.2). In line with the theoretical formulation of the learner criterion in the DML approach, we observe that the causal estimation performance depends on the validity of structural form assumptions such as sparsity and linearity. For example, in linear settings (i.e., DGP 1, 3 or 16) lasso performs well in terms of the rRMSE for the causal estimate as well as the empirical coverage. We believe that the reason why the AutoML learner performs well is its ability to adapt to various settings.

A lower combined nuisance loss is associated with better causal estimation. Low signal-to-noise ratios create challenges in small samples. In our simulation study, we investigate the relationship of the predictive performance for the nuisance functions, η_0, and the quality of the resulting causal estimate. A practical strategy for selecting the learners which would be aligned with the theoretical reasoning would be to pick the learner with the smallest out-of-sample loss for the nuisance predictions. In our simulations, however, we noticed that greedily minimizing the combined loss might not always deliver the lowest error (bias) on the causal parameter. We provide more insights on this in Appendix B.

As we compare tuned algorithms, for most DGPs we only observe an area of combined loss, where the fit is sufficient for a good causal inference performance. Still, considering the plots in Appendix E.4, it is valid to say that the possibility of a high bias decreases with a low combined loss. Considering the different scenarios of the ACIC data, it is important to relate the predictive performance for the nuisance function, η_0, to the noise in the prediction problems. Whenever it is possible to approximate η_0 relatively well, it is possible to obtain an accurate causal estimator. However, the ability to find such a predictive model depends on the noisiness of the incorporated predictive tasks, see the information in Table 2. This is further highlighted by Figure 5, which illustrates the relationship of the average bias and the combined predictive loss for increasing samples based on the BCH DGP: The larger the n/p-ratio, the higher is the predictive quality of the nuisance estimators in terms of the combined loss. The scatter plots also include the comparison to the default settings for the parameters of lasso and xgboost, which basically implement untuned learners. With increasing sample size, it is easier to detect the default parameter learners by considering their higher combined nuisance loss. It can be observed that the estimation quality with respect to θ_0 is worse for these learners. The results for the tuned estimators show a similar performance in terms of the combined nuisance loss as well

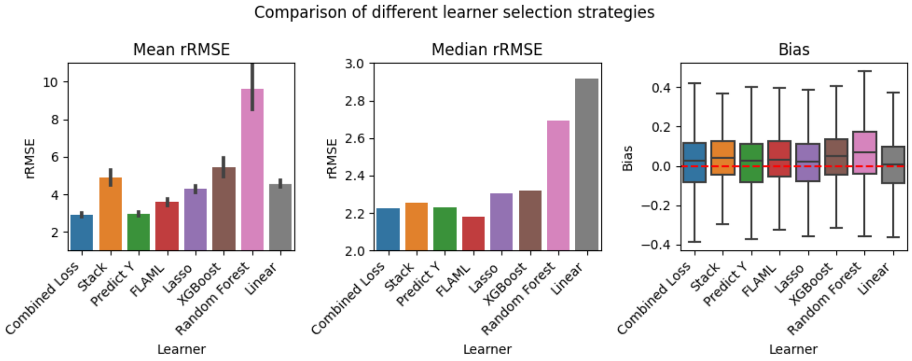

Figure 6: rRMSE of ATE parameter aggregated over learners and learner selection strategies for the *full sample* tuning scheme.

as the bias of the causal estimator.

Combined nuisance loss serves as a good learner selection metric for causal estimation. We briefly evaluate practical selection strategies for the employed learners based on the ACIC data. To do so, we focus on the *full sample* scheme and pick the causal model with the lowest predictive loss on Y (see Section 4.3). We investigate the following approaches: (1) Pick the single best learner for each data set based on the best predictive performance for Y, (2) Pick the single best learner for each iteration based on the combined out-of-sample nuisance loss, (3) Stack all tuned learners. We present average results for the rRMSE as well as a boxplot for the bias as aggregated over all DGP in Figure 6. It is visible that using the learner with the lowest combined loss leads to the best overall rRMSE (mean). The strategies that select using the predictive error on Y or always using *FLAML* appear to perform also well, especially concerning the median rRMSE. The performance of basic stacking (Wolpert, 1992) is overall competitive in terms of the median rRMSE, but is affected by a weak performance of random forest in several scenarios (high mean rRMSE). The linear/logistic benchmark model exhibits an overall inferior performance as compared most other learners.

4.3. Causal Models

In this section we assess the relationship of the structural assumptions encoded in the causal models (IRM and PLR) and the predictive performance of these models. As described in Section 2.1, the PLR model incorporates stronger structural assumptions than the IRM. Hence, in cases where these assumptions hold in the underlying DGP, we expect the PLR to benefit from that additional structure in terms of better estimation performance as compared to IRM estimates. However, in cases with a non-additive heterogeneous causal effect, the PLR estimate on θ_0 will be biased due to model misspecification. For our investigation, we split the DGPs into two categories: DGPs with a linear, additive effect and in DGPs with a heterogenous effect.[7] The results in Figure 7(a) are in line with our expectations, i.e., in linear additive DGPs, the PLR performs better than the IRM as it exhibits a lower rRMSE on average. Figure 7(b) illustrates that violations of these assumptions lead to a bias and, thus, less precise estimation of the ATE with the PLR. In contrast, the IRM is found to still

[7] We drop some DGPs, in which we observe both models struggle with the estimation, i.e. because model assumptions (conditional exogeneity) fail.

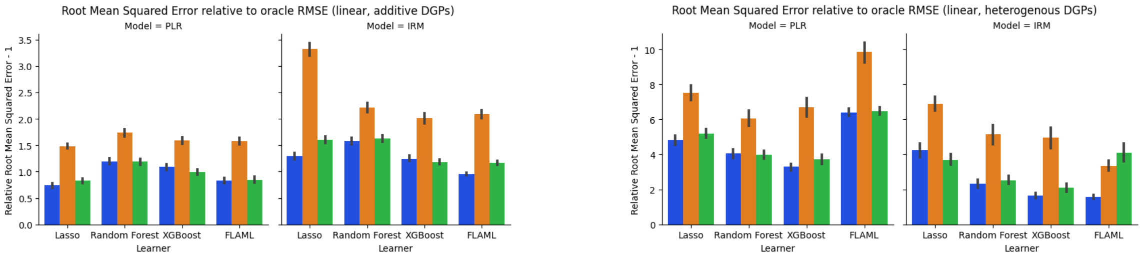

(*a*)

(*b*)

Figure 7: Root mean squared error on the ATE parameter, relative to oracle and subtracted by -1. The groups show the learner, the colors the tuning scheme. Results are aggregated over different groups of DGP. The columns show the two different causal models. (a) Aggregated over group of linear, additive processes. (b) Aggregated over group of interactive processes.

accurately estimate θ_0. These results hold generally for all considered learners.

The predictive performance of the causal models provides guidance on the choice of the causal model. In practice, researchers are typically concerned with the question of which causal model to choose when multiple models are basically applicable, i.e., to what extent one is willing to make the assumption of a constant treatment effect. We investigate whether the predictive performance of the causal models with regard to the outcome variable Y might be informative for that choice. To do so, we first estimate the causal model and then, generate predictions for the outcome variable Y as based on the PLR model (i.e., plugging in the observed values for D which are multiplied by the estimate $\hat{\theta_0}$) and the IRM (using predictions as generated by $g(D, X)$), see Table 4. The results are displayed in Figure 8. We find that in many of the settings, the relative advantage in the error predicting Y is associated with a better estimation performance for the causal parameter θ_0. However, as displayed in Table 14 presented in Appendix D, this measure does not always prove reliable. In the group of linear, additive DGPs, only in 46.33% of the iterations, the predictive loss using the PLR was lower, although it would yield the lower rRMSE on θ in overall nearly 80% . In terms of the IRM, this is a bit more straight forward: In 78.5% of the cases, the predictive loss accurately points towards the better causal model to use (see Table 15). These results can be interpreted to reflect a conservative modeling approach. The prediction-based selection of the causal rather tends to recommend the more general IRM unless there is stronger evidence for validity of the PLR assumptions.

5. Application

We apply the tuning methodology to the infant health and development program (IHDP) semi-synthetic data, which was previously used as a benchmark of causal ML methods in Chernozhukov et al. (2022) and Shi et al. (2019), see Appendix C.1 for more information. We use the IRM model and the full sample tuning approach, as well as `FLAML`, as this combination has performed well in our ACIC analysis. The results are displayed in Table 3. It is visible that the standard DML approach is very competitive with other state-of-the art appraoches such as RieszNets and DragonNet of Shi et al. (2019).

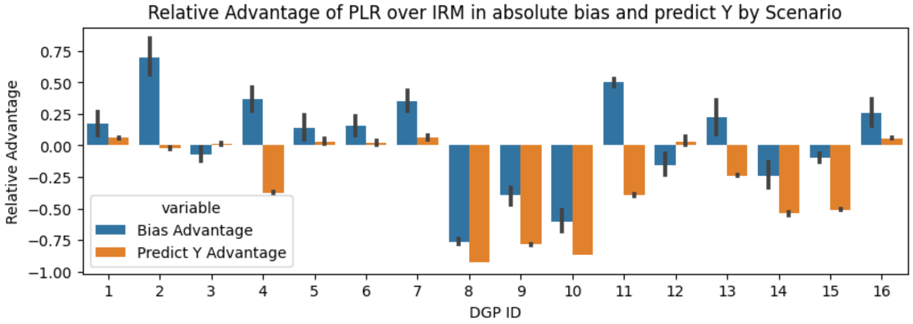

Figure 8: Relative advantage (or disadvantage) of PLR over IRM for all 16 ACIC processes. In many cases, the mean relative advantage in prediction error on the outcome Y coincides with the mean relative advantage in estimation of θ.

Method	MAE ± std. err.
DML with FLAML	0.111 ± 0.009
RieszNet (Chernozhukov et al., 2021)	0.110 ± 0.003
Dragonnet (Shi et al., 2019)	0.146 ± 0.010

Table 3: Comparison of the tuning strategies discussed in this work and other recent approaches.

6. Conclusion

Our results underscore the importance of proper hyperparameter tuning and selection of the ML estimators and the proper choice of DML related parameters. Particularly, the use of default parameter estimators can lead to significant bias in the causal estimate. Hence, we would like to encourage analysts working with causal and double machine learning approaches to transparently communicate their tuning strategies as well as information on the nuisance prediction loss, in particular when also employing several ML learners for nuisance estimation. Our results show that in general, tuning on the full data or on the folds is preferable over splitting the sample. In larger samples the difference of these approaches is found to vanish. Moreover, the choice between PLR and IRM was crucial in our results to achieve a low causal estimation error. To find the proper causal model, monitoring the predictive performance of the nuisance learners on Y can serve as a helpful guidance for the choice of the causal model. Finally, we generally find evidence supporting a relationship between the out-of-sample prediction error in the nuisance components and the error on the target parameter. This is in line with theoretic results. However, our results also suggest the measure of combined loss can be noisy, especially when dealing with small sample sizes and low signal-to-noise ratios. In our study, the lowest nuisance prediction error did not always translate in the optimal ML configuration for DML.

References

Philipp Bach, Victor Chernozhukov, Malte S Kurz, Martin Spindler, and Sven Klaassen. Doubleml–an object-oriented implementation of double machine learning in r. *arXiv preprint arXiv:2103.09603*, 2021.

Philipp Bach, Victor Chernozhukov, Malte S. Kurz, and Martin Spindler. Doubleml - an object-oriented implementation of double machine learning in python. *Journal of Machine Learning Research*, 23(53):1–6, 2022. URL http://jmlr.org/papers/v23/21-0862.html.

Alexandre Belloni, Victor Chernozhukov, and Christian Hansen. Inference on Treatment Effects after Selection among High-Dimensional Controls†. *The Review of Economic Studies*, 81(2):608–650, 11 2013. ISSN 0034-6527. doi: 10.1093/restud/rdt044. URL https://doi.org/10.1093/restud/rdt044.

Bernd Bischl, Martin Binder, Michel Lang, Tobias Pielok, Jakob Richter, Stefan Coors, Janek Thomas, Theresa Ullmann, Marc Becker, Anne-Laure Boulesteix, Difan Deng, and Marius Lindauer. Hyperparameter optimization: Foundations, algorithms, best practices and open challenges, 2021. URL https://arxiv.org/abs/2107.05847.

Bernd Bischl, Martin Binder, Michel Lang, Tobias Pielok, Jakob Richter, Stefan Coors, Janek Thomas, Theresa Ullmann, Marc Becker, Anne-Laure Boulesteix, et al. Hyperparameter optimization: Foundations, algorithms, best practices, and open challenges. *Wiley Interdisciplinary Reviews: Data Mining and Knowledge Discovery*, 13(2):e1484, 2023.

Leo Breiman. Random forests. *Machine learning*, 45:5–32, 2001.

Tianqi Chen and Carlos Guestrin. XGBoost: A scalable tree boosting system. In *Proceedings of the 22nd ACM SIGKDD International Conference on Knowledge Discovery and Data Mining*, KDD '16, pages 785–794, New York, NY, USA, 2016. ACM. ISBN 978-1-4503-4232-2. doi: 10.1145/2939672.2939785. URL http://doi.acm.org/10.1145/2939672.2939785.

Victor Chernozhukov, Denis Chetverikov, Mert Demirer, Esther Duflo, Christian Hansen, Whitney Newey, and James Robins. Double/debiased machine learning for treatment and structural parameters. *The Econometrics Journal*, 21(1):C1–C68, 2018. doi: 10.1111/ectj.12097.

Victor Chernozhukov, Whitney K. Newey, Victor Quintas-Martinez, and Vasilis Syrgkanis. Riesznet and forestriesz: Automatic debiased machine learning with neural nets and random forests, 2022.

Nitai Fingerhut, Matteo Sesia, and Yaniv Romano. Coordinated double machine learning. In *International Conference on Machine Learning*, pages 6499–6513. PMLR, 2022.

Michael C Knaus. Double machine learning-based programme evaluation under unconfoundedness. *The Econometrics Journal*, 25(3):602–627, 06 2022. doi: 10.1093/ectj/utac015. URL https://doi.org/10.1093%2Fectj%2Futac015.

Michael C Knaus, Michael Lechner, and Anthony Strittmatter. Machine learning estimation of heterogeneous causal effects: Empirical Monte Carlo evidence. *The Econometrics Journal*, 24(1): 134–161, 06 2020. ISSN 1368-4221. doi: 10.1093/ectj/utaa014. URL https://doi.org/10.1093/ectj/utaa014.

Divyat Mahajan, Ioannis Mitliagkas, Brady Neal, and Vasilis Syrgkanis. Empirical analysis of model selection for heterogenous causal effect estimation. *arXiv preprint arXiv:2211.01939*, 2022.

Yusuke Narita, Shota Yasui, and Kohei Yata. Off-policy bandit and reinforcement learning, 2020.

Gabriel Okasa. Meta-learners for estimation of causal effects: Finite sample cross-fit performance, 2022.

F. Pedregosa, G. Varoquaux, A. Gramfort, V. Michel, B. Thirion, O. Grisel, M. Blondel, P. Prettenhofer, R. Weiss, V. Dubourg, J. Vanderplas, A. Passos, D. Cournapeau, M. Brucher, M. Perrot, and E. Duchesnay. Scikit-learn: Machine learning in Python. *Journal of Machine Learning Research*, 12:2825–2830, 2011.

Philipp Probst, Anne-Laure Boulesteix, and Bernd Bischl. Tunability: Importance of hyperparameters of machine learning algorithms. *The Journal of Machine Learning Research*, 20(1):1934–1965, 2019.

James M Robins, Andrea Rotnitzky, and Lue Ping Zhao. Estimation of regression coefficients when some regressors are not always observed. *Journal of the American statistical Association*, 89(427): 846–866, 1994.

Oliver Schacht, Sven Klaassen, Philipp Schwarz, Martin Spindler, Daniel Grunbaum, and Sebastian Imhof. Causally learning an optimal rework policy. In Thuc Le, Jiuyong Li, Robert Ness, Sofia Triantafillou, Shohei Shimizu, Peng Cui, Kun Kuang, Jian Pei, Fei Wang, and Mattia Prosperi, editors, *Proceedings of The KDD'23 Workshop on Causal Discovery, Prediction and Decision*, volume 218 of *Proceedings of Machine Learning Research*, pages 3–24. PMLR, 07 Aug 2023. URL https://proceedings.mlr.press/v218/schacht23a.html.

Alejandro Schuler, Michael Baiocchi, Robert Tibshirani, and Nigam Shah. A comparison of methods for model selection when estimating individual treatment effects. *arXiv preprint arXiv:1804.05146*, 2018.

Claudia Shi, David M. Blei, and Victor Veitch. Adapting neural networks for the estimation of treatment effects, 2019.

Ezequiel Smucler, Andrea Rotnitzky, and James M Robins. A unifying approach for doubly-robust

$$\backslash$$

ell_1 $regularizedestimationofcausalcontrasts.$ *arXiv preprint arXiv:1904.03737*, 2019.

Robert Tibshirani. Regression shrinkage and selection via the lasso. *Journal of the Royal Statistical Society Series B: Statistical Methodology*, 58(1):267–288, 1996.

Mark J. van der Laan and Daniel Rubin. Targeted maximum likelihood learning. *The International Journal of Biostatistics*, 2(1), 2006. doi: doi:10.2202/1557-4679.1043. URL https://doi.org/10.2202/1557-4679.1043.

Chi Wang and Qingyun Wu. FLO: fast and lightweight hyperparameter optimization for automl. *CoRR*, abs/1911.04706, 2019. URL http://arxiv.org/abs/1911.04706.

David H Wolpert. Stacked generalization. *Neural networks*, 5(2):241–259, 1992.

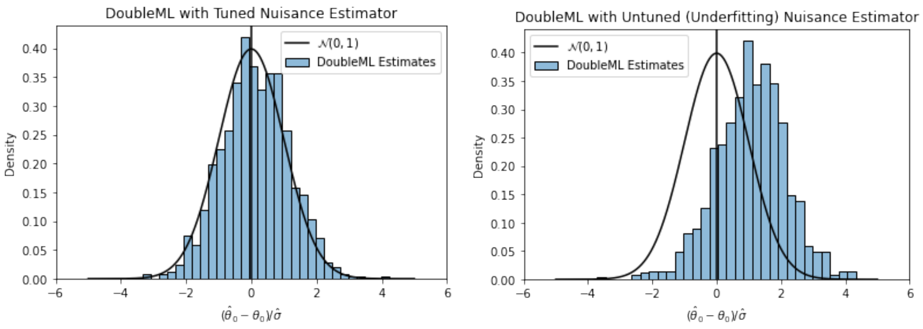

(*a*) (*b*)

Figure 9: Histogram of studentized DML estimator corresponding to a properly tuned ML estimator in Panel (a) and to an underfitting learner in Panel (b).

Appendix A. Motivation for Hyperparameter Tuning for Double Machine Learning

Figure 9 highlights the importance of appropriately choosing the ML predictors using a simulated data from a data generating process (DGP) from Chernozhukov et al. (2018) with 1000 repetitions. The left plot shows the empirical distribution corresponding to a DML estimate on θ_0 when estimating the nuisance with optimally tuned ML methods (random forest). The distribution of the studentized estimator is close to a normal distribution. However, the right figure shows the analogous results for regression stumps, which implies underfitting of the nuisance components, η_0. Even though a Neyman-orthogonal scoring function as well as sample-splitting are used in the DML procedure, the causal estimate exhibits a severe bias and thus the inference becomes invalid.

Appendix B. Additional Information on Learner Selection

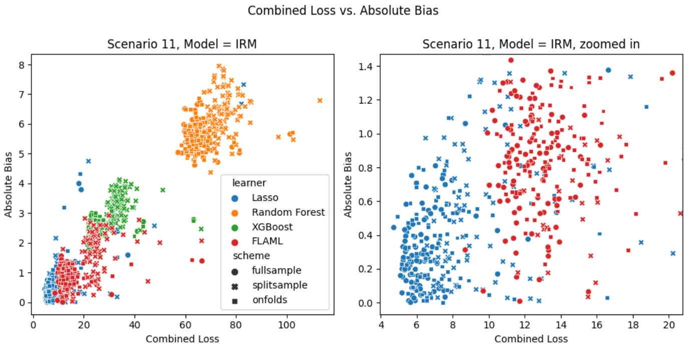

Figure 10: Absolute bias on causal estimate and combined loss of nuisance prediction for DGP 11 in IRM model.

As motivated in Section 4.2, based on our results, we find it not straight forward to select the best learner and tuning scheme purely on the combined nuisance loss. We showcase this in Figure

Name of Metric	Explanation
Relative root mean squared error (rRMSE)	$\sqrt{\frac{MSE(\hat{\theta})}{MSE(\hat{\theta}_{oracle})}}$. The rRMSE was used as a metric in the ACIC 2019 challenge.
rRMSE-1	We subtract the rRMSE by one for clearer barplots.
Mean bias	$\bar{\theta} = \frac{1}{R}\sum_r^R(\hat{\theta}_r - \theta)$ with $r = 1, ..., R$ being the repetitions.
Standard deviation	$s = \sqrt{\frac{1}{R-1}\sum_r^R(\hat{\theta}_r - \bar{\theta})^2}$
Coverage	The coverage of the estimated 95% confidence band with the true parameter.
Predictive loss	$MSE(\hat{Y})$. In case of an IRM, this is equivalent to the out-of-sample loss of $\hat{g}_0(D, X)$. In case of an PLR, this is $\frac{1}{n}\sum_i^n(Y_i - \hat{\theta}D_i - \hat{\ell}(X_i))^2$.
Combined loss	We combine the out-of-sample error for the prediction of both nuisance components. Identically to Chernozhukov et al. (2018), we use for the PLR $RMSE(\hat{m}_0) \cdot \Big(RMSE(\hat{m}_0) + RMSE(\hat{\ell}_0)\Big)$ and for the IRM $RMSE(\hat{m}_0) \cdot RMSE(\hat{g}_0)$. This serves a measure to assess the overall quality of predictive fit for the nuisance function.

Table 4: Overview of metrics used in the analysis of the results.

10 for scenario 11, in which tuning of the nuisance estimators is particularly important, as the signal-to-noise ratio is high. On the left panel, we see that there is clearly a relationship that a lower combined loss implies a lower absolute bias. In the group of very well fitted learners (right panel), this difference becomes marginal and random statistical deviations are becoming more important.

Appendix C. Information on Metrics and ACIC 2019 Competition

Based on the learnings from above, we pick the tuning scheme, learner and causal model with different approaches to compare our results to the results of some selected top challenge participants. *Strategy 1* refers to the most sophisticated strategy: Per each repitition first selecting the causal model by the lowest median of MSE on Y, then selecting learner and tuning scheme by the lowest combined loss. *Always FLAML* uses the AutoML tuning on the fullsample. *Untuned RF* is a comparison to the straight-away approach to always use the more flexible model (IRM) with Random Forest in standard hyperparameter configurations.

Approach	**Relative Bias**	**RRMSE**	**Coverage**	**Rel. Std.**
Strategy 1	1372.1 (10)	2.932 (11)	0.813 (7)	2.407 (16)
Always `FLAML`	1457.1 (15)	2.971 (13)	0.815 (8)	2.441 (17)
Untuned RF	1735.0 (17)	9.256 (16)	0.665 (17)	2.559 (12)
*BART**	1628.8 (11)	2.257 (3)	0.750 (15)	1.244 (1)
*Std**	1105.0 (9)	3.428 (9)	0.821 (5)	2.509 (11)
*BART TMLE**	1301.5 (2)	2.192 (1)	0.811 (8)	1.356 (4)
*eb**	988.04 (1)	3.567 (15)	0.850 (2)	2.748 (21)

Table 5: Data challenge results for selected tuning strategies. Approaches marked with an * are original challenge participants. The number in parenthesis is the rank of that method in the competition. The ranks were assigned on a weighted average on the scenarios, which explains deviations between the absolute mean and the rank.

C.1. Information on IHDP Benchmark

IHDP was a randomized control trial, studying the effect of certain measures (i.e. attendance at specialized clinics) of low birth weight infants on future developmental and health outcomes. We use 1000 generated datasets of 747 observations as in Chernozhukov et al. (2022). Each observation consists of an outcome Y, a binary treatment T and 25 confounders X that can are continuous or binary.

Appendix D. Full Results in Tables

D.1. Results for ACIC in PLR

Learner		FLAML			Lasso			Random Forest			XGBoost		Linear
Scheme	Full Sample	On Folds	Split Sample	Full Sample	On Folds	Split Sample	Full Sample	On Folds	Split Sample	Full Sample	On Folds	Split Sample	Full Sample
DGP #													
1	1.0956	**1.0711**	1.5503	1.0950	1.0834	1.5079	1.1037	1.1243	1.5464	1.1211	1.1007	1.5178	1.1316
2	1.2170	**1.1127**	1.9287	1.3736	1.3645	1.9830	1.5906	1.6105	2.1073	1.4099	1.4231	1.7750	1.2233
3	2.5519	2.7523	3.0255	1.8610	1.9886	2.6898	2.6640	2.6650	2.9801	2.6569	2.7180	3.0301	**1.2472**
4	1.5408	1.2863	2.0526	1.2975	1.7261	2.5651	1.9560	1.9304	2.2321	1.7138	1.6899	2.1581	**1.2317**
5	5.8245	7.4997	11.1874	5.2938	4.9919	10.2095	4.7933	4.0252	8.1064	**3.9275**	4.5782	5.6138	7.7705
6	5.2872	**5.2690**	7.2466	6.3771	6.6130	9.1519	6.5917	6.5087	7.9793	6.5679	6.2539	8.2382	6.0200
7	1.9908	1.9907	3.0353	2.7420	2.7849	3.1009	2.7755	2.6055	3.6463	3.1572	2.6295	3.6171	**1.7489**
8	11.5467	10.6801	8.0848	7.2969	7.2996	8.0905	6.2807	6.1882	6.7360	6.8165	6.8931	8.3904	**5.9193**
9	7.0943	6.0958	11.1786	4.7796	5.7621	7.5124	2.5647	**2.4356**	3.6759	2.7096	2.7590	4.1712	6.3971
10	4.7436	4.5514	7.4038	1.9442	1.9287	2.6623	2.9929	3.0181	2.8375	**1.8525**	1.8546	2.4634	5.1557
11	8.3446	**5.5440**	15.8245	9.0712	9.7453	12.9054	73.4896	73.7701	88.6298	28.7352	29.0876	32.8459	28.2037
12	7.2101	9.9652	22.9163	10.8196	10.4065	17.0188	9.7530	9.5929	17.2773	**7.0729**	9.1706	18.9174	10.5871
13	1.5778	1.5353	2.6675	1.1738	1.2183	2.5256	1.3325	1.3368	2.0142	**1.1345**	1.1930	1.7841	1.2574
14	6.4037	6.0266	4.6313	4.1826	5.6041	7.2586	3.6332	3.6325	4.7675	2.9706	**2.9178**	4.4545	7.3758
15	2.3446	2.4324	3.7893	1.5638	**1.5424**	2.6860	8.3167	8.4921	8.8339	3.4202	3.4428	4.2264	1.6678
16	2.6017	2.8543	3.8674	2.0663	**2.0125**	3.0523	3.0596	3.1965	3.9160	2.4614	2.3995	3.4155	2.3445

Table 6: Relative Root Mean Squared Error of estimates

Learner		FLAML			Lasso			Random Forest			XGBoost		Linear
Scheme	Full Sample	On Folds	Split Sample	Full Sample	On Folds	Split Sample	Full Sample	On Folds	Split Sample	Full Sample	On Folds	Split Sample	Full Sample
DGP #													
1	**0.0008**	0.0014	0.0162	-0.0149	-0.0144	-0.0059	0.0045	0.0034	0.0196	0.0021	0.0105	0.0242	0.0131
2	**0.0123**	0.0152	0.0976	0.0627	0.0624	0.0878	0.0872	0.0866	0.1187	0.0684	0.0662	0.0873	0.0226
3	0.1690	0.1863	0.1879	0.1097	0.1220	0.1467	0.1777	0.1788	0.1817	0.1778	0.1809	0.1874	**0.0357**
4	-0.0029	0.0099	-0.0310	0.0351	0.0636	0.1096	0.0886	0.0880	0.0905	0.0738	0.0721	0.0843	-0.0000
5	-0.0583	**0.0043**	0.0699	-0.0783	-0.0678	-0.0977	-0.0719	-0.0741	-0.0355	-0.0955	-0.0671	-0.1006	-0.0123
6	-0.0958	-0.0843	-0.2166	-0.2132	-0.2548	-0.2739	-0.2598	-0.2628	-0.2685	-0.2194	-0.2587	-0.2809	**0.0104**
7	0.0746	0.0753	0.1127	0.1097	0.1141	0.1248	0.1181	0.1156	0.1514	0.1062	0.1029	0.1372	**0.0572**
8	0.1565	0.1466	0.1090	0.1011	0.1005	0.0972	0.0865	0.0850	0.0898	0.0946	0.0958	0.1152	**0.0729**
9	-0.5722	-0.5066	-0.8890	-0.3237	-0.4878	-0.5670	-0.0850	-0.0764	-0.1858	-0.1461	-0.1567	-0.2578	-0.5376
10	-0.5134	-0.5120	-0.7648	-0.1604	-0.1790	-0.2061	-0.3251	-0.3273	-0.2509	-0.1731	-0.1712	-0.1875	-0.5848
11	-0.1500	-0.0640	-0.3808	0.3297	0.3569	0.2032	3.9828	3.9992	4.7878	1.5458	1.5690	1.7544	-1.5191
12	0.4234	0.5158	0.7573	0.5785	0.5916	0.7617	0.5461	0.5479	0.6864	**0.3640**	0.4289	0.6427	0.4687
13	0.0449	0.0428	0.0752	**0.0156**	0.0195	0.0316	0.0316	0.0333	0.0461	0.0228	0.0254	0.0369	0.0228
14	-7.3964	-7.0113	-4.6878	-4.0059	-6.1637	-7.5730	-3.7727	-3.7802	-4.3082	-3.0428	-2.9528	-3.8826	-8.5521
15	0.0473	0.0503	0.0787	0.0034	**0.0022**	0.0023	0.2065	0.2106	0.2158	0.0797	0.0797	0.0944	0.0226
16	-0.1057	-0.1172	-0.1450	-0.0676	-0.0633	-0.0740	0.0744	0.0871	0.0936	-0.0177	-0.0207	-0.0245	-0.1177

Table 7: Mean Bias of Estimates in PLR

Learner		FLAML			Lasso			Random Forest			XGBoost		Linear
Scheme	Full Sample	On Folds	Split Sample	Full Sample	On Folds	Split Sample	Full Sample	On Folds	Split Sample	Full Sample	On Folds	Split Sample	Full Sample
DGP #													
1	0.1453	**0.1420**	0.2050	0.1445	0.1430	0.1999	0.1463	0.1491	0.2041	0.1487	0.1456	0.1998	0.1495
2	0.0847	0.0767	0.0936	0.0731	0.0725	0.1079	**0.0695**	0.0724	0.0878	0.0713	0.0747	0.0887	0.0829
3	0.0815	**0.0789**	0.1192	0.0819	0.0807	0.1330	0.0823	0.0799	0.1226	0.0809	0.0847	0.1207	0.0848
4	0.0848	0.0701	0.1086	0.0621	0.0703	0.0884	0.0605	0.0589	0.0826	**0.0583**	0.0583	0.0833	0.0678
5	0.5001	0.6484	0.9646	0.4509	0.4261	0.8772	0.4080	0.3399	0.6999	**0.3257**	0.3900	0.4747	0.6717
6	0.3675	0.3690	0.4730	0.4050	0.4002	0.5971	0.3951	0.3859	0.5058	0.4172	**0.3664**	0.5202	0.4324
7	0.0689	0.0681	0.1060	0.0866	0.0845	0.0970	0.0778	**0.0652**	0.1077	0.1211	0.0859	0.1232	0.0685
8	0.0496	0.0394	0.0364	0.0233	0.0260	0.0617	0.0223	0.0225	0.0332	0.0209	**0.0206**	0.0311	0.0422
9	0.3541	0.2784	0.5781	0.3181	0.2459	0.4320	0.2287	0.2188	0.2959	0.2121	**0.2102**	0.3009	0.2809
10	0.2472	0.1911	0.4545	0.1703	0.1474	0.2454	0.1534	0.1560	0.2314	**0.1402**	0.1429	0.2297	0.2032
11	0.4316	0.2969	0.7780	0.3704	0.3955	0.6770	0.4368	0.4274	0.6540	0.2552	**0.2312**	0.3603	0.2387
12	**0.5901**	0.8615	2.1833	0.9240	0.8655	1.5371	0.8168	0.7960	1.6010	0.6127	0.8187	1.7961	0.9587
13	0.0445	0.0442	0.0759	0.0444	0.0448	0.0963	0.0430	0.0419	0.0663	**0.0394**	0.0406	0.0613	0.0450
14	3.0356	2.7291	3.3949	3.3609	3.3169	4.9907	2.5251	2.5123	4.1216	**2.1265**	2.1395	3.9963	3.4142
15	0.0361	0.0357	0.0552	0.0397	0.0392	0.0683	0.0420	0.0438	0.0595	**0.0341**	0.0356	0.0508	0.0359
16	0.0972	0.1052	0.1567	0.0920	0.0914	0.1516	0.1519	0.1537	0.1952	0.1350	0.1311	0.1874	**0.0533**

Table 8: Standard Deviation of Estimates in PLR

Learner		FLAML			Lasso			Random Forest			XGBoost		Linear
Scheme	Full Sample	On Folds	Split Sample	Full Sample	On Folds	Split Sample	Full Sample	On Folds	Split Sample	Full Sample	On Folds	Split Sample	Full Sample
DGP #													
1	0.9800	0.9700	0.9900	**0.9500**	0.9600	0.9700	0.9700	0.9700	0.9900	0.9600	0.9600	0.9900	0.9600
2	0.8900	0.9200	0.8800	0.8200	0.8400	0.8600	0.7700	0.7200	0.8300	0.8600	0.8200	0.8800	**0.9400**
3	0.4800	0.3600	0.6800	0.7500	0.6400	0.7400	0.3100	0.3800	0.7100	0.3900	0.3700	0.6400	**0.8500**
4	0.8500	0.9100	0.9000	0.9000	0.7700	0.7800	0.6900	0.7100	0.8000	0.8000	0.7800	0.8500	**0.9300**
5	0.9800	**0.9400**	0.9800	**0.9400**	**0.9600**	**0.9600**	0.9800	0.9700	0.9900	0.9700	0.9900	0.9900	**0.9600**
6	0.9300	0.9300	0.9800	0.8700	0.8700	0.8900	0.8700	0.8800	**0.9600**	0.9300	0.8900	0.9100	0.9100
7	0.8000	0.6900	0.7500	0.5600	0.5400	0.6900	0.5000	0.5100	0.6100	0.6300	0.6100	0.6800	**0.8600**
8	0.0000	0.0000	0.1900	0.0500	0.0500	0.1800	0.0700	0.0900	0.3500	0.0300	0.0300	0.1000	**0.4600**
9	0.3800	0.4100	0.3600	0.6800	0.4200	0.6500	0.8700	**0.9100**	**0.9100**	0.8400	0.8300	0.8600	0.3900
10	0.1900	0.0800	0.2300	0.7100	0.7400	**0.7900**	0.4000	0.3500	0.6800	0.7500	0.7400	0.7600	0.0600
11	0.6600	**0.8500**	0.5900	0.5700	0.5100	0.5800	0.0000	0.0000	0.0000	0.0000	0.0000	0.0000	0.0000
12	0.5600	0.6600	0.6500	0.7100	0.6400	0.7200	0.6200	0.5900	0.8000	0.7700	0.7800	0.8200	**0.8600**
13	0.7700	0.8100	0.7600	0.9400	0.9300	**0.9500**	0.9000	0.9100	0.8500	0.9300	0.9200	0.9300	0.9400
14	0.1400	0.1800	0.6200	0.6300	0.4100	0.5300	0.5400	0.5500	**0.7200**	0.6400	0.6900	0.6900	0.1800
15	0.7500	0.7100	0.6900	0.9800	0.9800	**0.9600**	0.0000	0.0000	0.0700	0.4000	0.4500	0.5900	0.9200
16	0.7700	0.7300	0.7900	0.9100	0.9200	0.9200	0.9300	0.9200	0.9300	**0.9500**	**0.9500**	0.9300	0.5100

Table 9: Coverage of a 95% confidence interval of Estimates in PLR

D.2. Results for ACIC in IRM

Learner		FLAML			Lasso			Random Forest			XGBoost		Linear
Scheme	Full Sample	On Folds	Split Sample	Full Sample	On Folds	Split Sample	Full Sample	On Folds	Split Sample	Full Sample	On Folds	Split Sample	Full Sample
DGP #													
1	1.3588	1.3630	1.7276	1.1518	1.1371	2.0895	1.1122	1.1045	1.4990	1.1264	**1.0896**	1.6069	2.5831
2	**1.8481**	1.9990	2.8468	2.2938	2.7010	4.9673	2.4966	2.5182	3.0464	1.9754	1.9987	2.6066	2.6247
3	2.1507	2.3604	2.7521	**1.9395**	2.3650	4.0566	2.6021	2.6391	2.9372	2.4988	2.4924	2.9337	2.3944
4	1.8834	1.9894	2.6970	**1.8346**	2.9436	3.7637	2.3158	2.3131	2.4912	2.1787	2.1952	2.4840	4.5590
5	5.2058	**2.9685**	4.7837	5.9087	5.2530	8.9381	3.5861	4.3097	7.6908	4.8240	4.1155	6.5163	14.1868
6	**6.0683**	9.4405	7.7748	7.2419	6.9156	42.8648	6.5744	6.3504	7.9838	6.1250	6.2455	7.8693	11.6220
7	2.1790	2.4775	3.7704	3.1105	3.4190	4.0870	3.3558	3.3924	4.8019	3.2628	2.8861	5.1730	**1.9411**
8	2.1816	2.1540	2.9889	2.3516	2.6188	4.9129	2.5738	2.5683	3.6972	**1.9341**	1.9384	2.8684	3.3512
9	2.1780	2.1648	3.1616	3.3264	3.5310	6.5262	2.2096	2.2212	3.3503	2.1566	**2.1208**	2.9709	6.0698
10	**1.0583**	1.1584	1.6751	1.2953	1.2360	1.6880	1.1315	1.1312	1.7191	1.0623	1.0628	1.7064	1.2540
11	16.1035	17.1417	30.9374	14.8590	14.1398	26.1562	102.4055	102.6740	117.7050	44.9960	45.1375	61.1337	**6.8687**
12	**5.0122**	17.5622	10.8482	13.3427	10.9391	14.3851	7.9385	8.8918	18.0516	6.0753	8.4058	19.1437	13.2814
13	1.2434	1.2850	2.4153	1.4954	1.5418	2.1832	1.5515	1.5889	2.2084	**1.2405**	1.2465	1.8756	1.9354
14	2.4035	2.4894	3.0314	5.8649	5.1529	11.8739	2.7362	2.8075	3.8439	**1.9560**	1.9653	3.0277	7.7059
15	1.8830	1.9021	3.0548	1.8549	1.8952	4.2829	7.1471	7.3370	7.6195	3.3580	3.3432	4.0278	**1.5976**
16	2.2907	2.8196	4.7231	3.4038	3.0508	6.9476	3.6034	3.7914	4.5298	2.4305	2.4160	3.2699	**1.5786**

Table 10: Relative Root Mean Squared Error in IRM

Learner		FLAML			Lasso			Random Forest			XGBoost		Linear
Scheme	Full Sample	On Folds	Split Sample	Full Sample	On Folds	Split Sample	Full Sample	On Folds	Split Sample	Full Sample	On Folds	Split Sample	Full Sample
DGP #													
1	**0.0017**	0.0132	0.0121	-0.0129	-0.0158	-0.0174	0.0038	0.0070	0.0184	0.0041	0.0156	0.0245	0.0061
2	0.0838	0.1014	0.1675	0.0932	0.1513	0.1754	0.1592	0.1607	0.1927	0.1183	0.1175	0.1545	**0.0294**
3	0.1160	0.1252	0.1573	0.0730	0.1269	0.1055	0.1734	0.1751	0.1788	0.1655	0.1640	0.1761	**0.0036**
4	0.0803	0.0908	0.1166	0.0693	0.1331	0.1139	0.1122	0.1128	0.1098	0.1043	0.1049	0.1096	**0.0091**
5	-0.0661	-0.0845	-0.1171	-0.1125	-0.0852	-0.0962	-0.0879	-0.0671	-0.0479	-0.0761	-0.0728	-0.0773	-0.0209
6	-0.1540	-0.0734	-0.2870	-0.1898	-0.3038	**0.0318**	-0.2756	-0.2828	-0.2810	-0.2699	-0.2814	-0.2962	-0.0363
7	0.0852	0.0931	0.1401	0.1210	0.1440	0.1477	0.1567	0.1578	0.2161	0.1274	0.1241	0.1864	**0.0533**
8	0.0156	0.0121	0.0305	0.0221	0.0223	0.0370	0.0305	0.0304	0.0438	0.0193	0.0201	0.0281	**0.0060**
9	-0.0592	-0.0859	-0.0950	-0.1448	-0.1583	-0.1980	-0.0969	-0.1024	-0.1718	-0.0811	-0.0843	-0.1317	-0.1616
10	-0.0384	-0.0357	-0.0057	-0.0143	-0.0219	0.0089	-0.0559	-0.0555	-0.0692	-0.0345	-0.0326	-0.0487	0.0134
11	0.7748	0.9012	1.4762	0.3106	0.3859	0.4988	5.5669	5.5815	6.3789	2.4396	2.4493	3.3038	-0.0109
12	**0.2658**	0.4442	0.3857	0.6121	0.6047	0.5671	0.3786	0.4018	0.5647	0.2879	0.3216	0.5837	0.4215
13	0.0239	0.0253	0.0273	0.0143	0.0210	**0.0075**	0.0470	0.0484	0.0595	0.0296	0.0296	0.0389	0.0183
14	-0.9836	-1.0578	-2.0111	-0.8780	-2.3449	-4.6327	-2.3683	-2.4044	-2.8725	-1.2906	-1.2137	-1.6891	2.3656
15	0.0285	0.0318	0.0430	-0.0035	-0.0075	-0.0080	0.1764	0.1809	0.1830	0.0782	0.0775	0.0894	0.0075
16	-0.0403	-0.0292	-0.0409	-0.0846	-0.0789	-0.0807	0.1266	0.1378	0.1451	0.0183	0.0198	0.0304	**0.0069**

Table 11: Mean Bias of Estimates in IRM

Learner		FLAML			Lasso			Random Forest			XGBoost		Linear
Scheme	Full Sample	On Folds	Split Sample	Full Sample	On Folds	Split Sample	Full Sample	On Folds	Split Sample	Full Sample	On Folds	Split Sample	Full Sample
DGP #													
1	0.1802	0.1803	0.2288	0.1522	0.1500	0.2766	0.1475	0.1463	0.1979	0.1493	**0.1437**	0.2117	0.3425
2	0.0989	0.0968	0.1083	0.1312	0.1137	0.3014	0.0720	0.0724	0.0913	**0.0717**	0.0761	0.0972	0.1821
3	0.1077	0.1205	0.1276	0.1229	0.1191	0.2800	0.0807	0.0836	0.1212	**0.0797**	0.0816	0.1247	0.1767
4	0.0651	0.0606	0.0911	0.0732	0.0915	0.1727	0.0595	**0.0580**	0.0815	0.0584	0.0591	0.0810	0.2508
5	0.4451	**0.2422**	0.3965	0.4982	0.4460	0.7667	0.2972	0.3664	0.6631	0.4100	0.3482	0.5580	1.2263
6	0.4076	0.6742	0.4784	0.4841	0.3920	3.0795	0.3826	0.3569	0.4993	**0.3465**	0.3484	0.4806	0.8342
7	0.0713	0.0854	0.1317	0.1025	0.0981	0.1471	**0.0682**	0.0702	0.1144	0.1070	0.0788	0.1867	0.0835
8	0.0270	0.0283	0.0297	0.0252	0.0299	0.0595	0.0202	0.0203	0.0291	0.0196	**0.0190**	0.0296	0.0475
9	0.1986	0.1871	0.2854	0.2812	0.2961	0.5885	0.1864	0.1847	0.2681	0.1884	**0.1832**	0.2499	0.5545
10	**0.1217**	0.1350	0.2020	0.1556	0.1474	0.2034	0.1244	0.1245	0.1953	0.1233	0.1239	0.1999	0.1507
11	0.4149	0.2484	0.8199	0.7519	0.6707	1.3426	0.4231	0.4249	0.7007	0.2573	**0.2383**	0.4411	0.3762
12	**0.4294**	1.7148	1.0236	1.1975	0.9214	1.3348	0.7048	0.8011	1.7307	0.5404	0.7841	1.8403	1.2713
13	0.0438	0.0449	0.0930	0.0583	0.0582	0.0874	0.0406	0.0413	0.0655	**0.0400**	0.0402	0.0644	0.0755
14	2.8469	2.9348	3.2191	7.3008	6.0159	14.1417	2.4709	2.5599	3.8595	**2.0815**	2.1411	3.3956	9.3652
15	0.0385	0.0364	0.0647	0.0471	0.0477	0.1087	0.0409	0.0426	0.0617	**0.0337**	0.0342	0.0494	0.0400
16	0.1201	0.1532	0.2581	0.1681	0.1491	0.3758	0.1535	0.1576	0.2039	0.1332	0.1322	0.1784	**0.0871**

Table 12: Standard Deviation of Estimates in IRM

Learner		FLAML			Lasso			Random Forest			XGBoost		Linear
Scheme	Full Sample	On Folds	Split Sample	Full Sample	On Folds	Split Sample	Full Sample	On Folds	Split Sample	Full Sample	On Folds	Split Sample	Full Sample
DGP #													
1	0.9800	0.9800	**0.9500**	**0.9500**	0.9800	0.9400	0.9800	0.9800	0.9900	0.9700	0.9800	0.9900	0.9800
2	0.8300	0.8300	0.6600	0.8400	0.6300	0.7800	0.4200	0.3900	0.5500	0.6100	0.5800	0.7000	**0.9700**
3	0.7600	0.7800	0.7600	0.8200	0.5900	0.8800	0.3900	0.3900	0.6900	0.4300	0.4500	0.6800	**0.9400**
4	0.7300	0.7500	0.8400	0.8300	0.4600	0.8200	0.5100	0.5400	0.7500	0.5700	0.5800	0.7500	**0.9500**
5	1.0000	0.9700	1.0000	0.9700	0.9800	0.9900	0.9700	0.9700	1.0000	0.9800	0.9700	0.9900	**0.9500**
6	0.9300	**0.9400**	0.9200	0.8900	0.8300	0.8900	0.8600	0.8500	0.9300	0.9100	0.9000	0.9100	**0.9600**
7	0.7700	0.7100	0.6800	0.6600	0.4700	0.6900	0.2500	0.2500	0.2800	0.4900	0.5100	0.5200	**0.9000**
8	0.9100	0.9100	0.8700	0.8300	0.8400	0.8000	0.7300	0.7300	0.7400	0.8400	0.8600	0.8400	**0.9600**
9	**0.9300**	0.9200	0.9700	0.9200	0.8800	**0.9300**	0.9000	0.9100	0.9200	0.8900	0.8900	0.9000	0.9700
10	0.9400	0.9200	**0.9500**	0.9400	**0.9500**	0.9100	0.8800	0.8700	0.8700	0.9200	0.9000	0.8700	**0.9500**
11	0.2200	0.0800	0.2900	0.8400	0.7200	0.7400	0.0000	0.0000	0.0000	0.0000	0.0000	0.0000	**0.9400**
12	0.9300	0.9600	0.9800	0.8600	0.7500	0.9000	0.8600	0.8300	0.9100	0.8800	0.8700	0.9600	**0.9500**
13	0.9200	0.9600	0.9400	0.9200	**0.9500**	0.9400	0.8500	0.8000	0.8300	0.8900	0.9000	0.9000	0.9200
14	0.9000	0.9300	0.8200	0.8800	0.7400	0.7900	0.7100	0.6700	0.8200	0.8300	0.8300	0.8600	**0.9600**
15	0.8600	0.8600	0.8300	0.9600	**0.9500**	0.9600	0.0100	0.0100	0.1300	0.4400	0.4300	0.6700	0.9600
16	0.9600	0.9200	0.9400	0.9600	0.9400	0.9400	0.8500	0.8100	0.8900	**0.9500**	0.9600	0.9600	**0.9500**

Table 13: Coverage of a 95% confidence interval of Estimates in IRM

	IRM θ	PLR θ
IRM Y_{loss}	11.91%	24.42%
PLR Y_{loss}	30.25 %	**33.42**%

Table 14: Share of iterations in which each model was better in estimating θ and the predictive loss on Y for the group of linear, additive DGP.

	IRM θ	PLR θ
IRM Y_{loss}	**75.65**%	5.95%
PLR Y_{loss}	15.75%	2.65%

Table 15: Share of iterations in which each model was better in estimating θ and the predictive loss on Y for the group of heterogeneous DGP.

Appendix E. Full Results in Figures

E.1. Relative Root Mean Squared Error

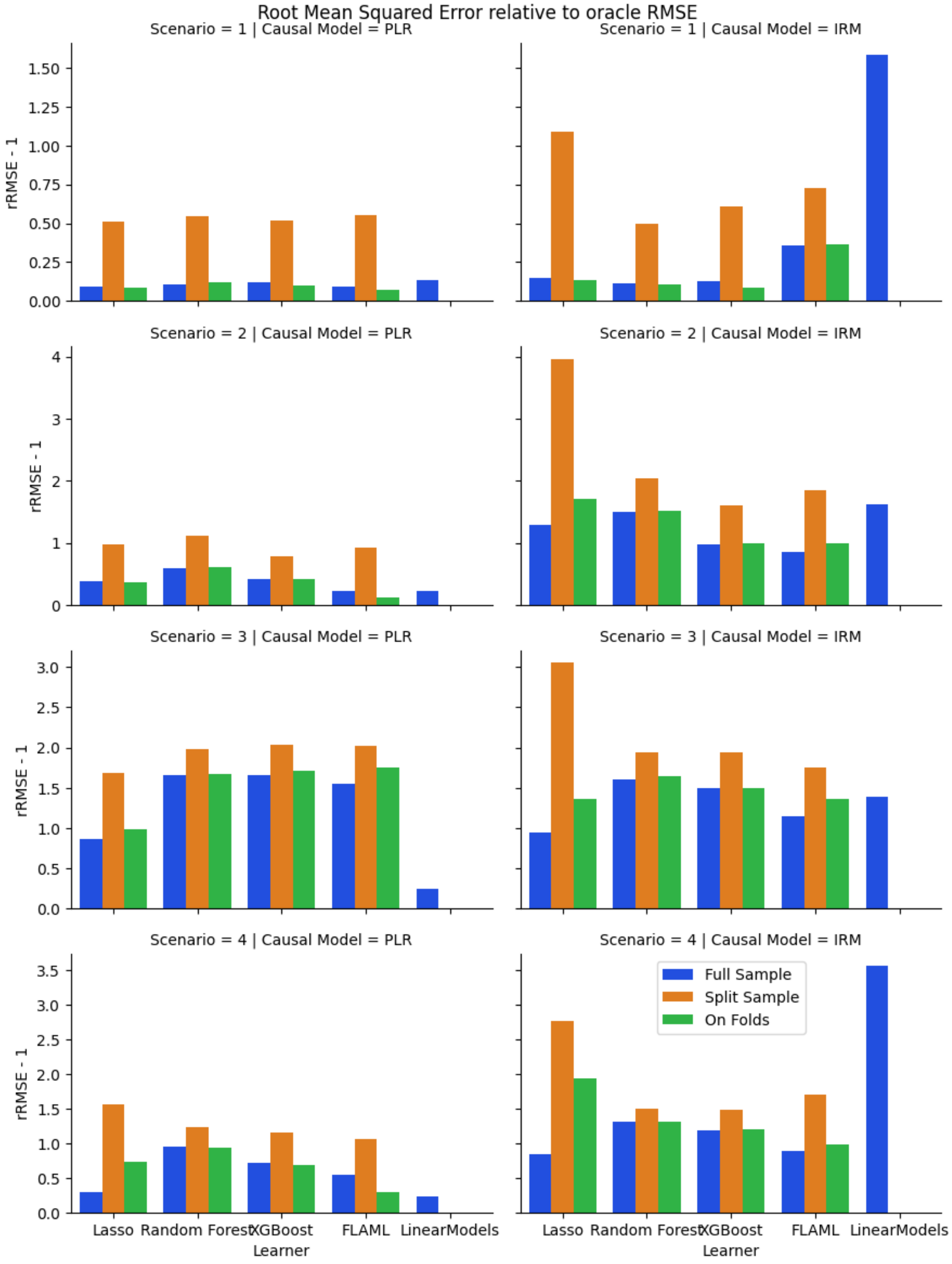

Figure 11: Relative Root Mean Squared Error of ACIC DGP 1-4 (adjusted by -1)

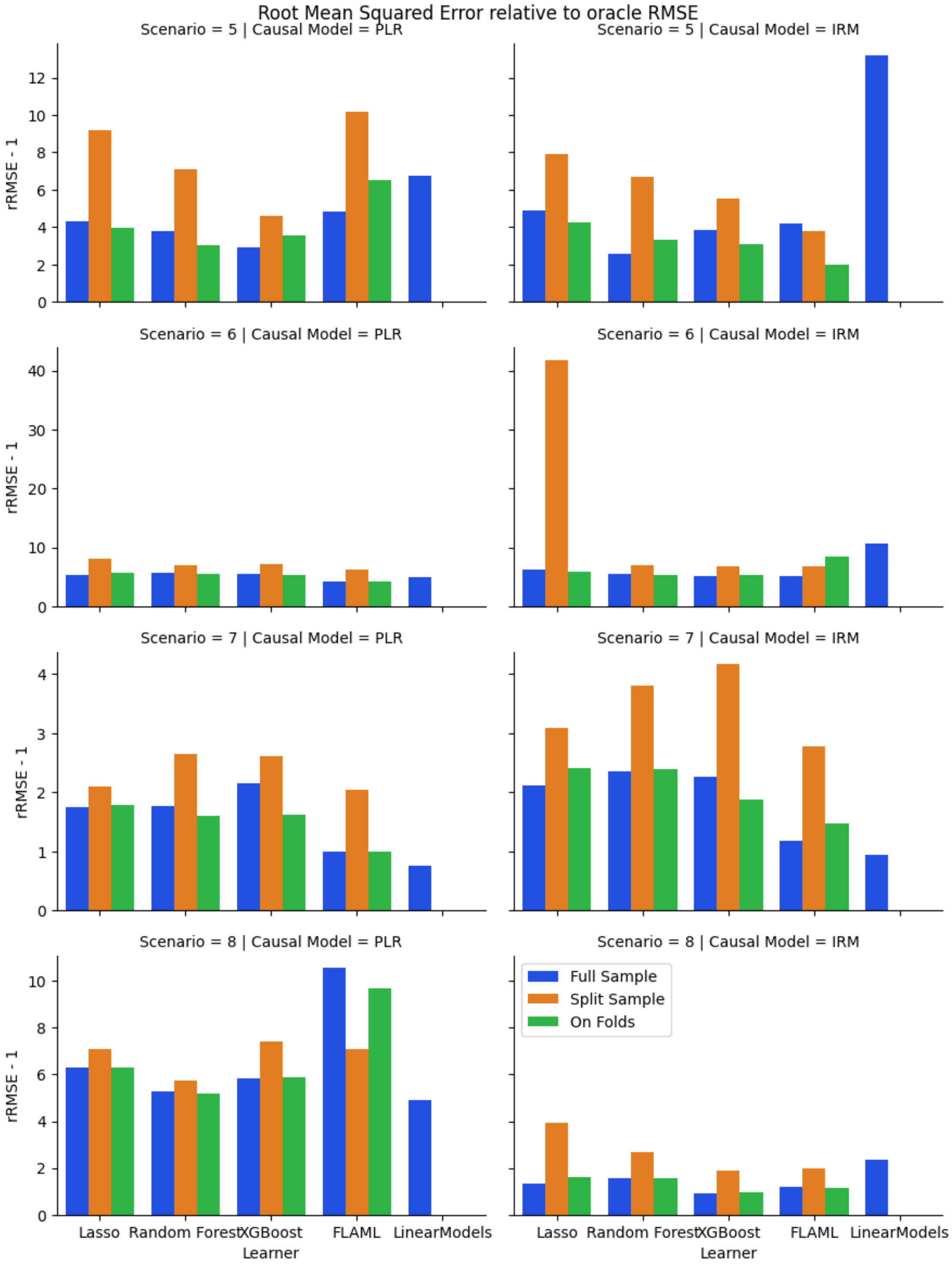

Figure 12: Relative Root Mean Squared Error of ACIC DGP 5-8 (adjusted by -1)

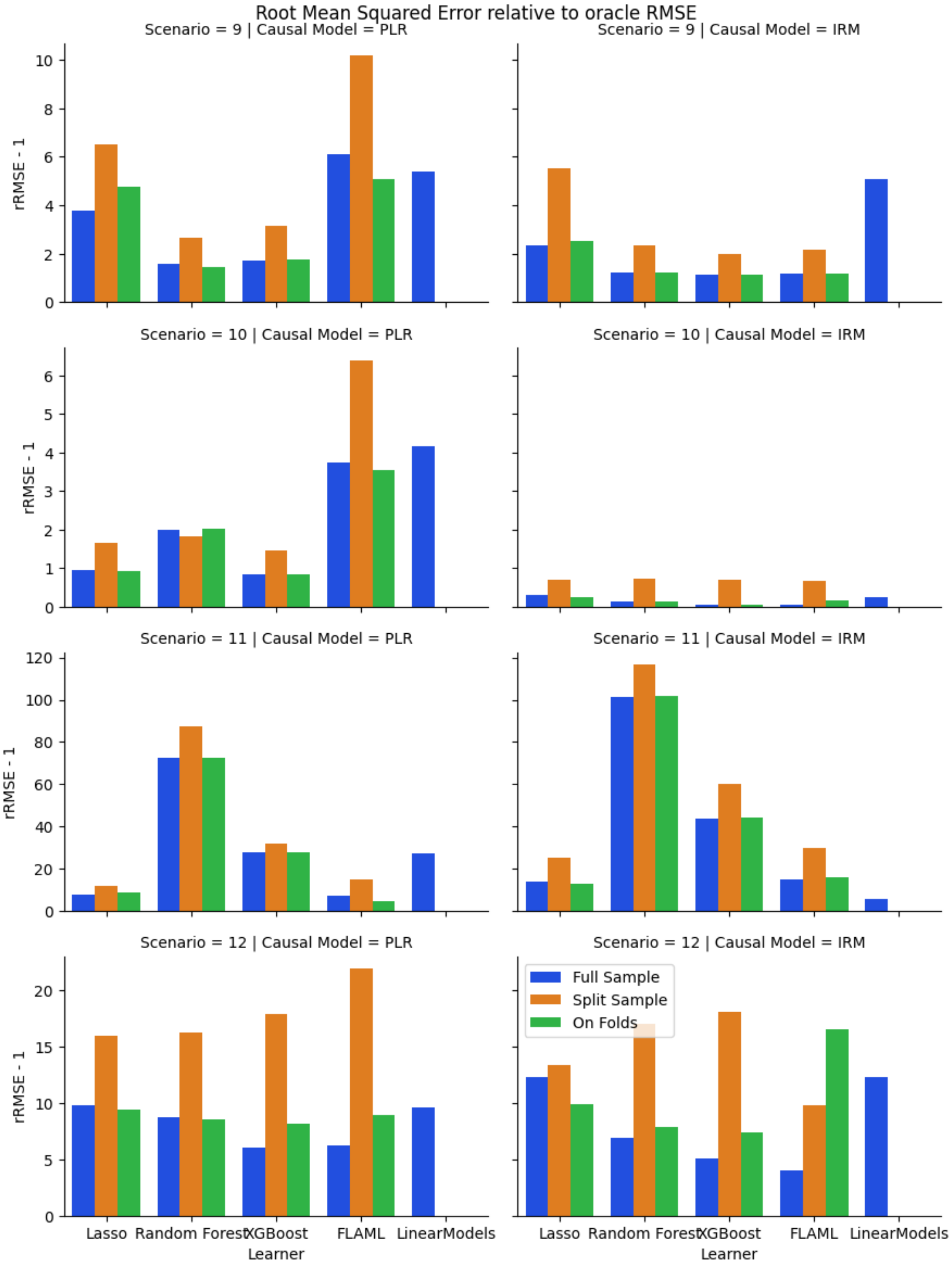

Figure 13: Relative Root Mean Squared Error of ACIC DGP 9-12 (adjusted by -1)

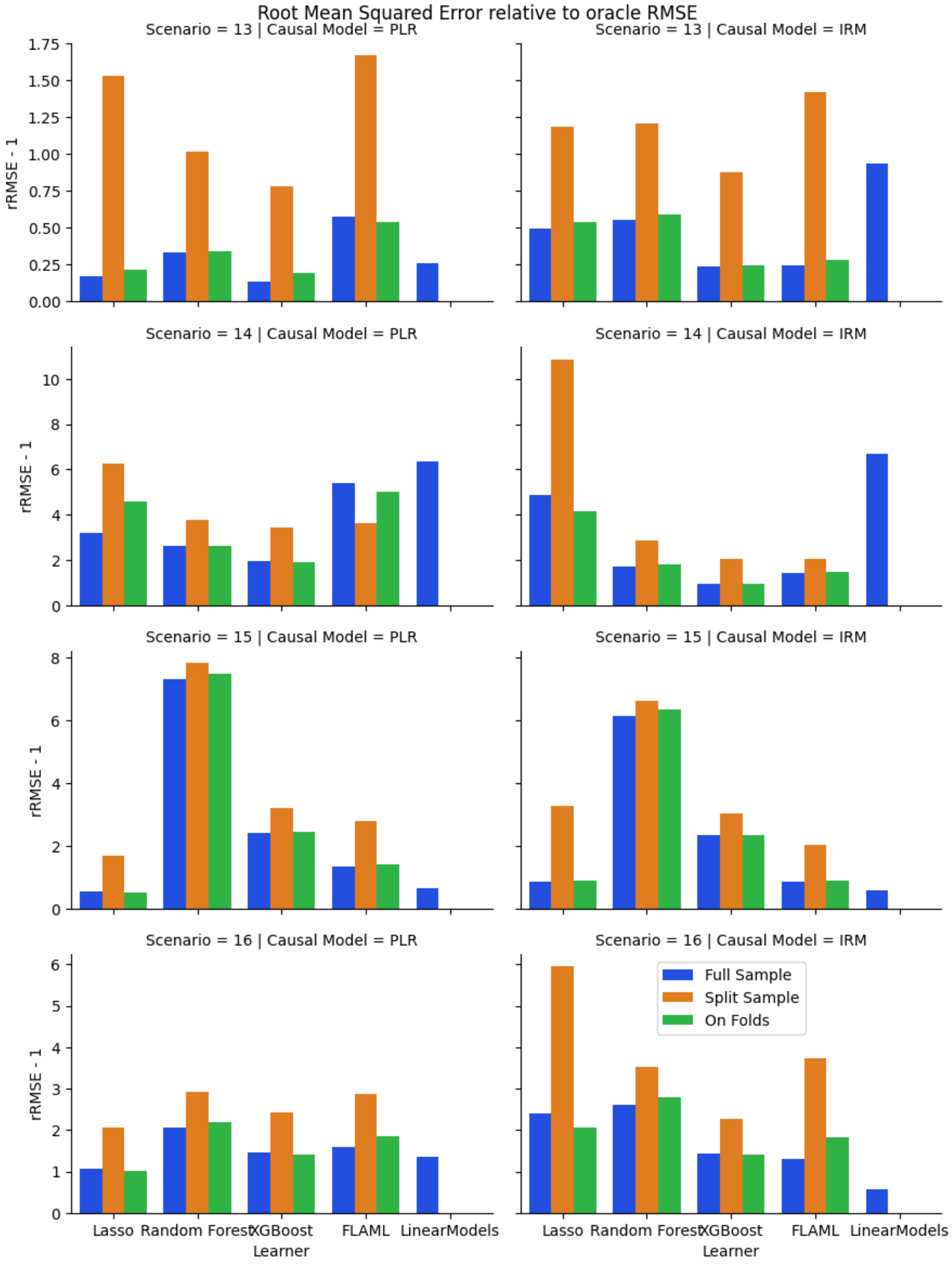

Figure 14: Relative Root Mean Squared Error of ACIC DGP 13-16 (adjusted by -1)

E.2. Bias of Estimates

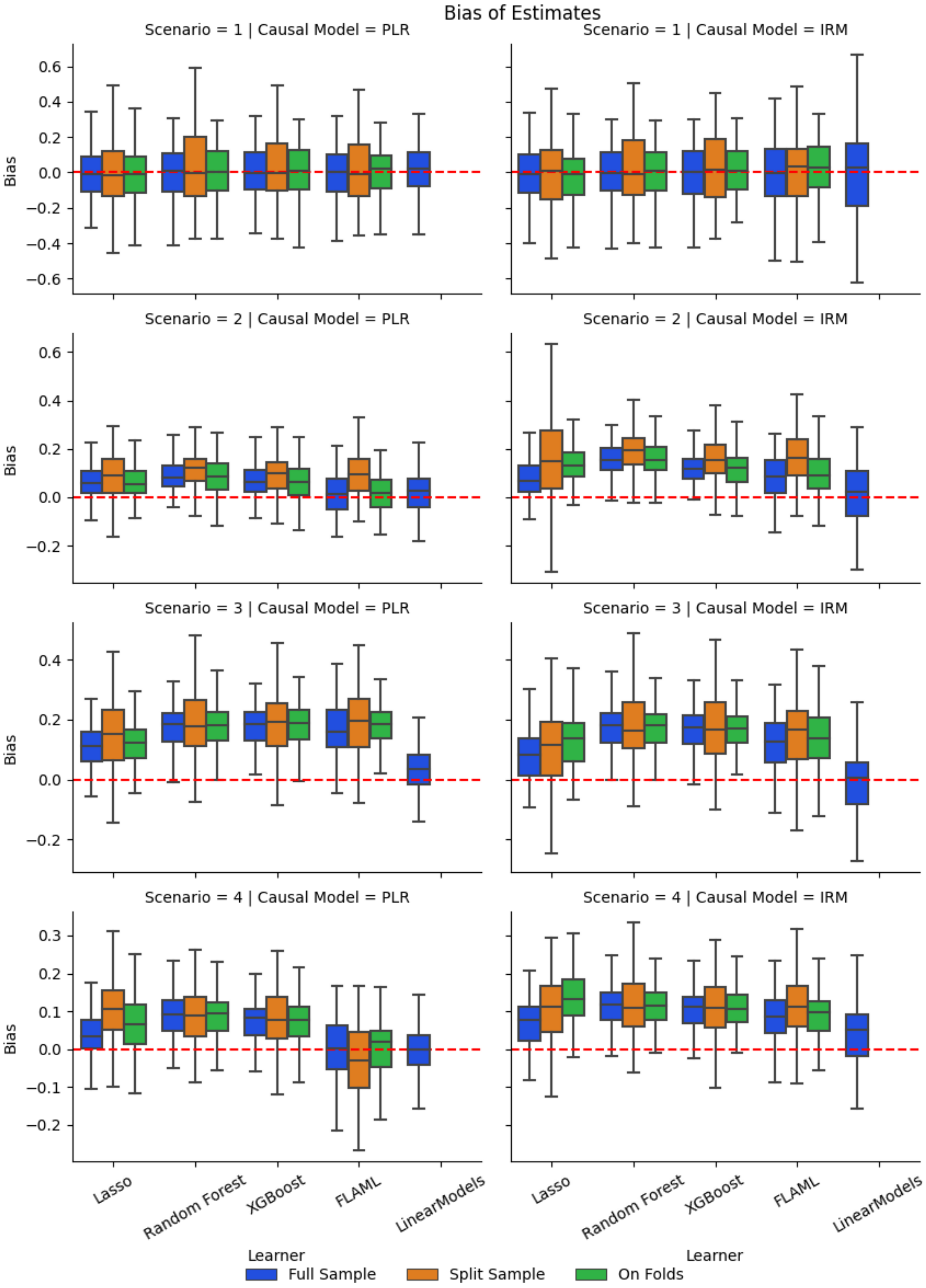

Figure 15: Boxplot of bias, ACIC DGP 1-4

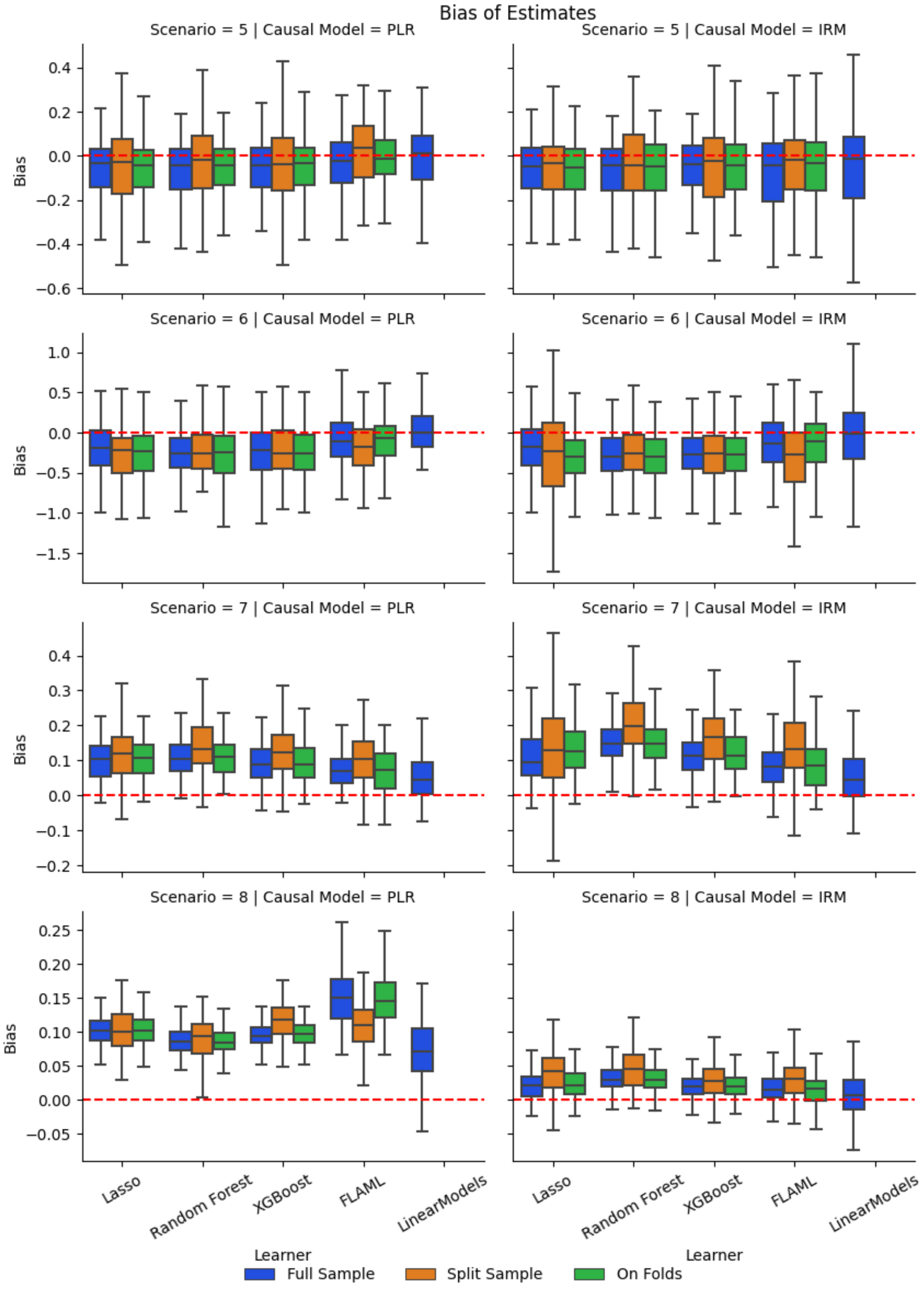

Figure 16: Boxplot of bias, ACIC DGP 5-8

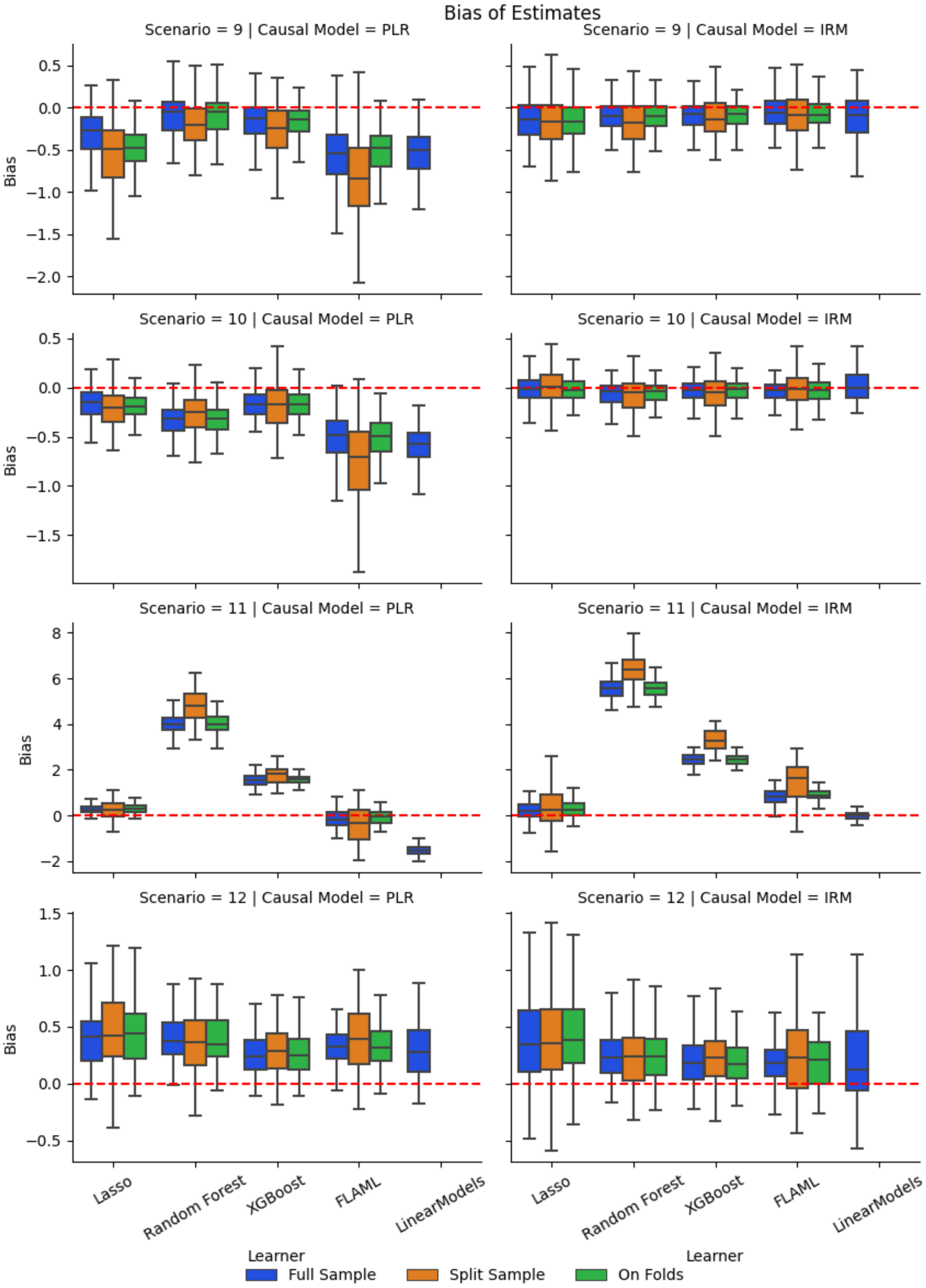

Figure 17: Boxplot of bias, ACIC DGP 9-12

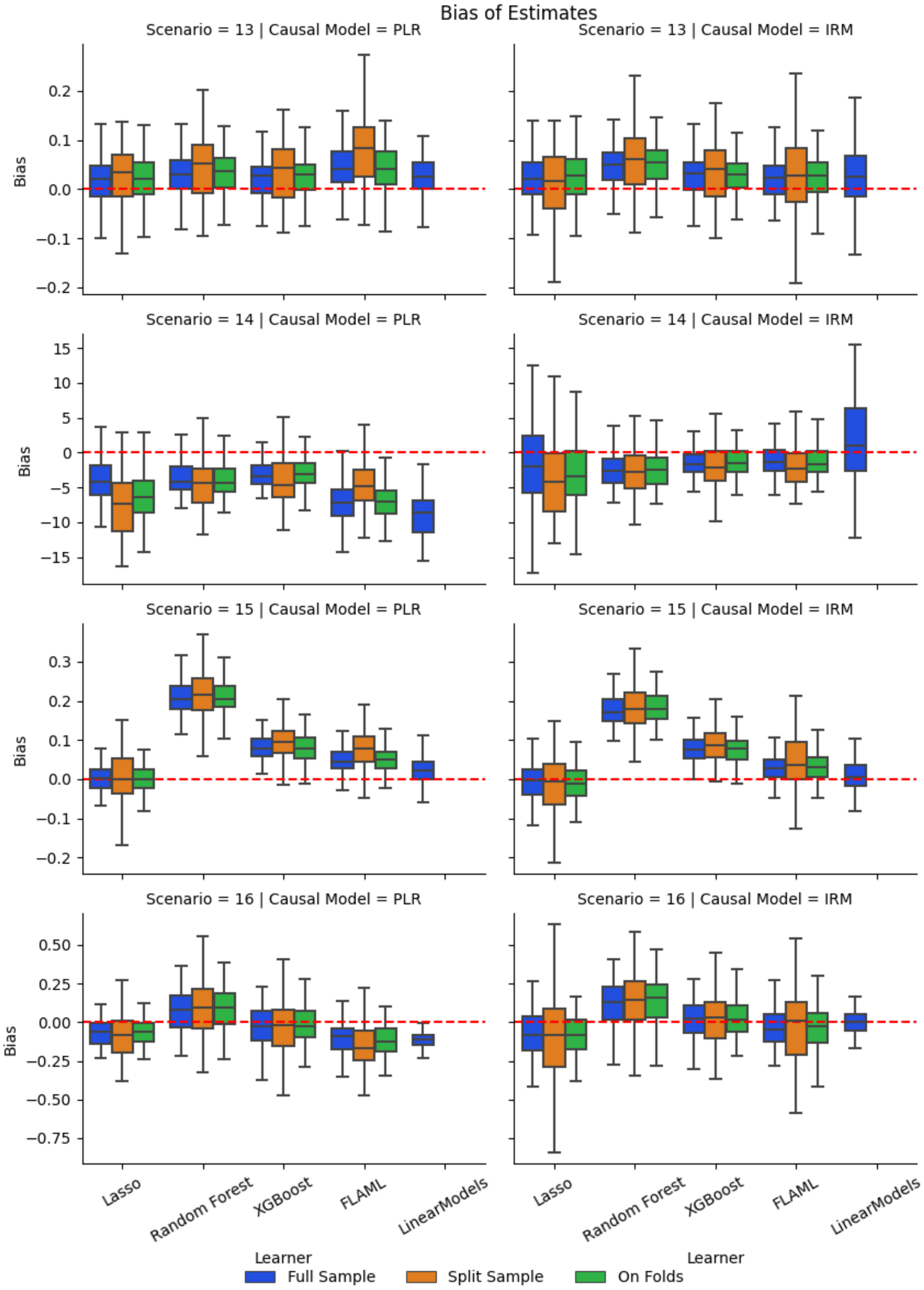

Figure 18: Boxplot of bias, ACIC DGP 13-15

E.3. Predictive Performance

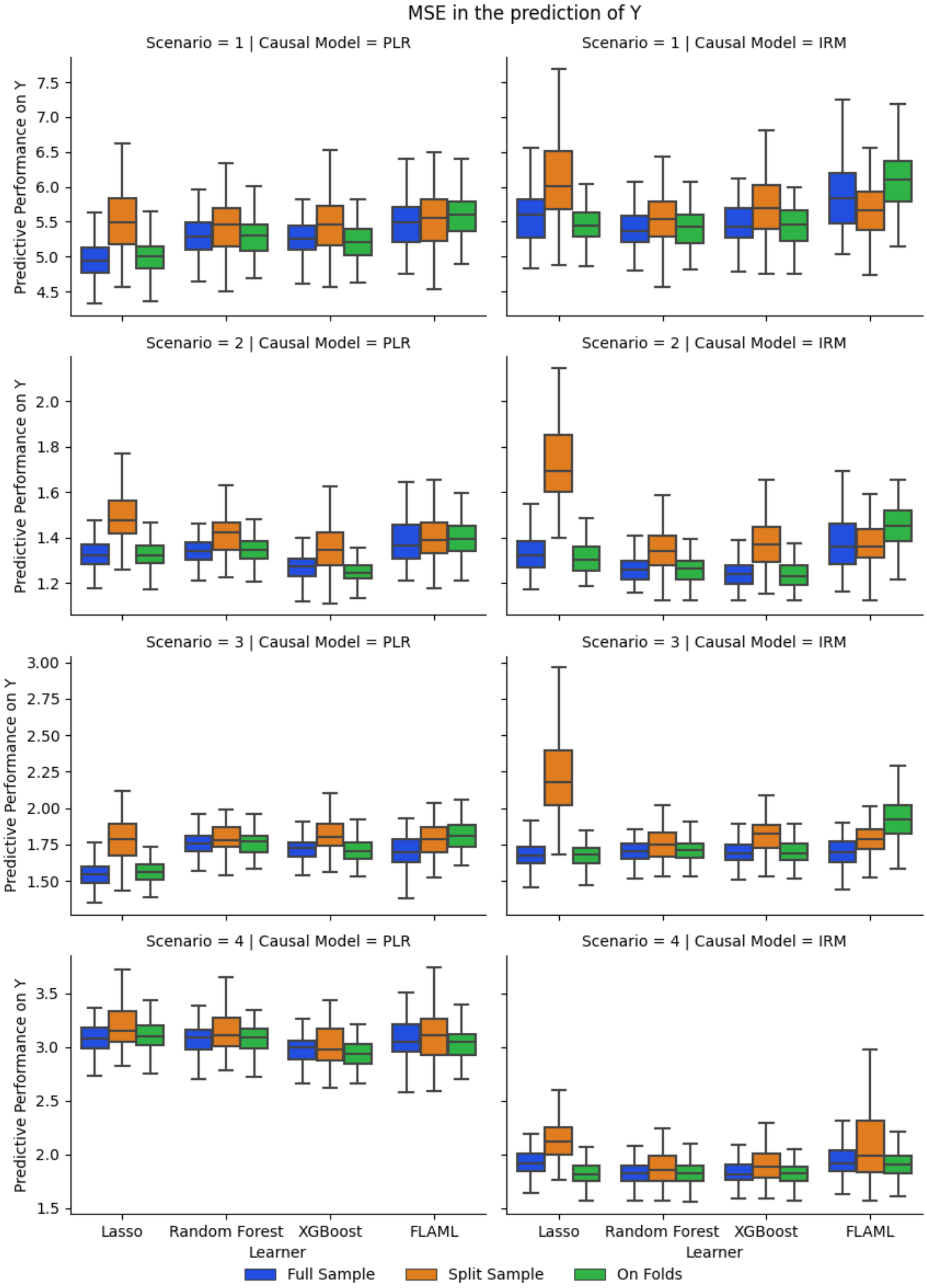

Figure 19: Predictive Performance on Y of ACIC DGP 1-4

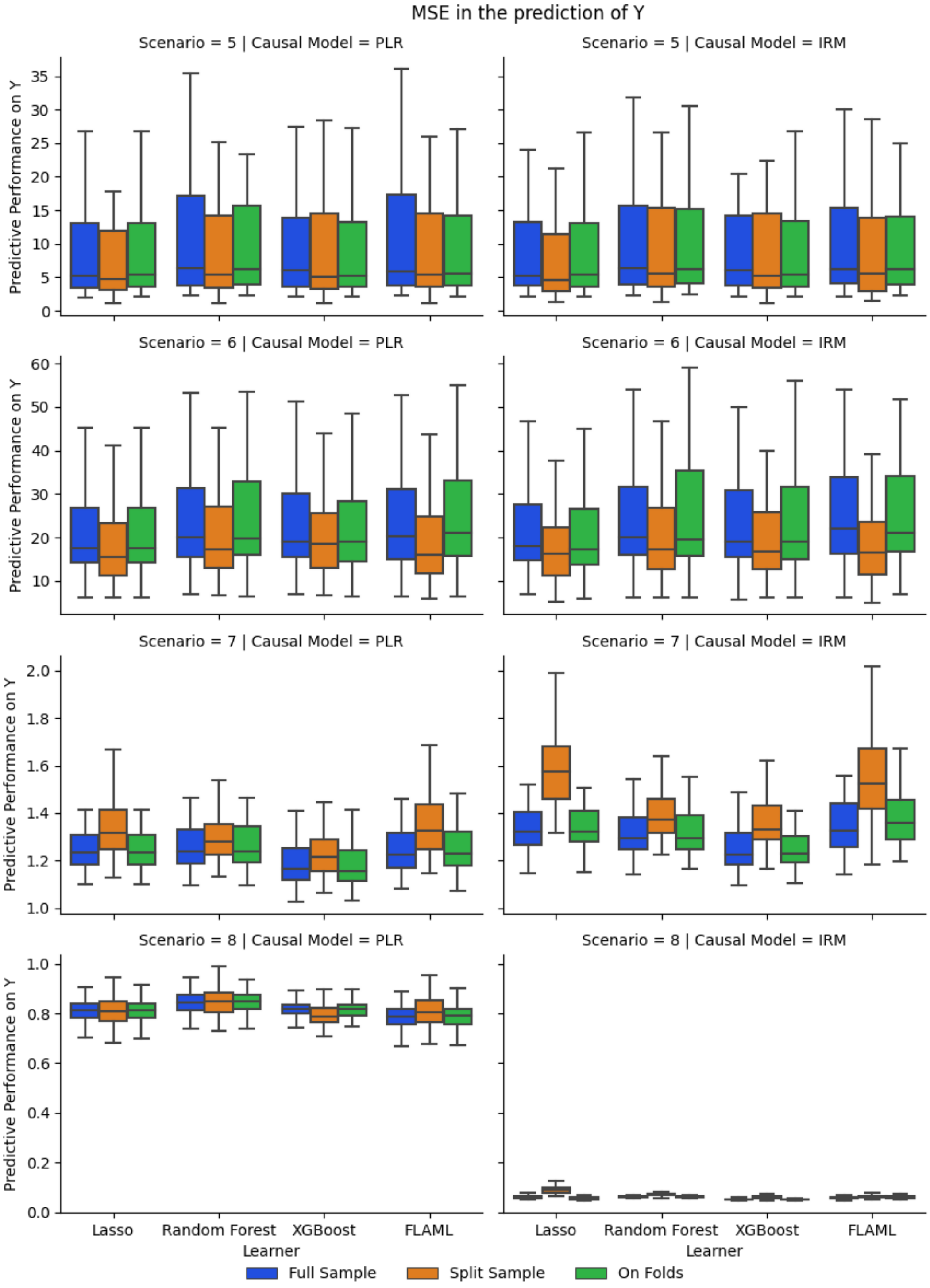

Figure 20: Predictive Performance on Y of ACIC DGP 5-8

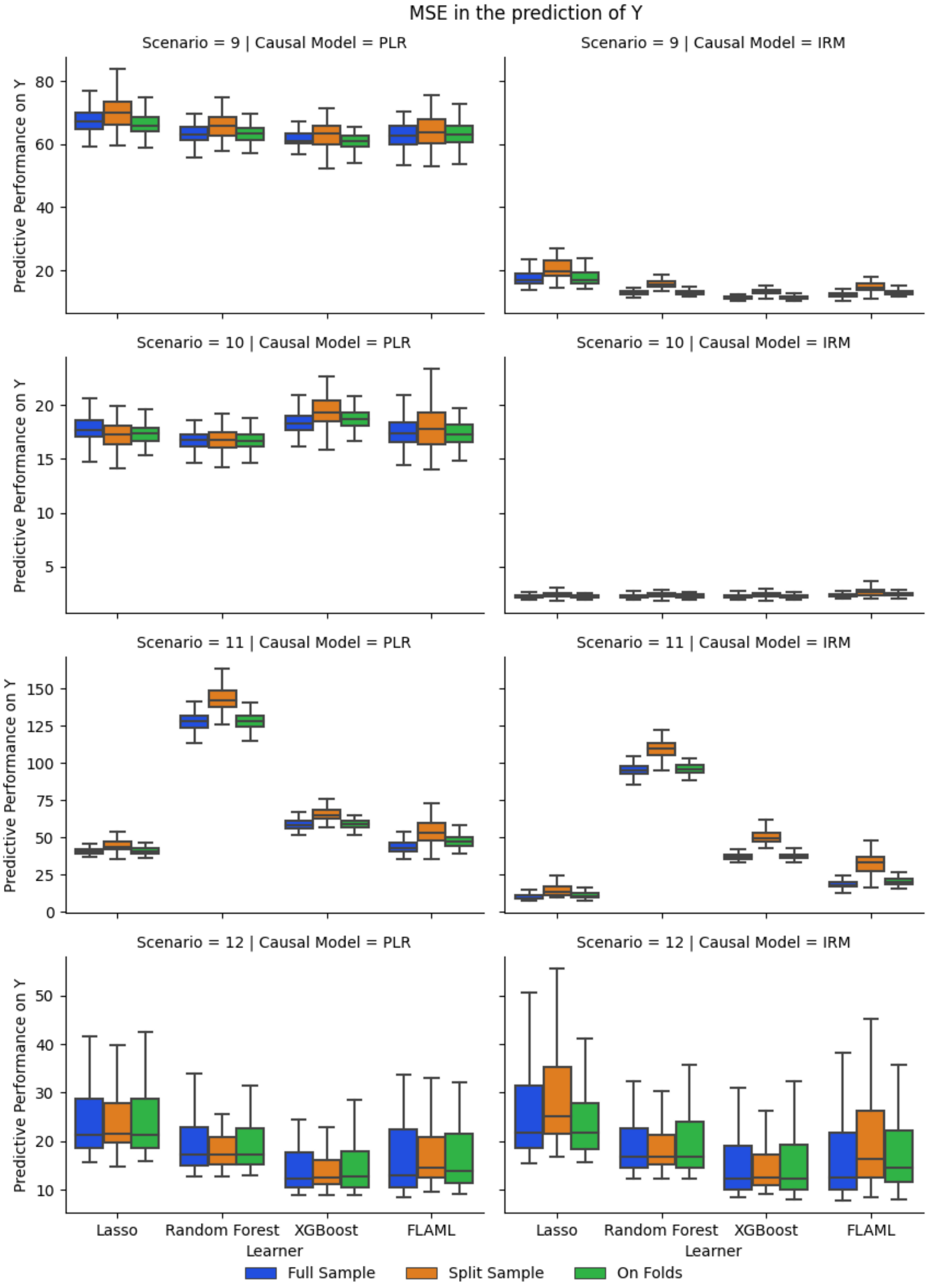

Figure 21: Predictive Performance on Y of ACIC DGP 9-12

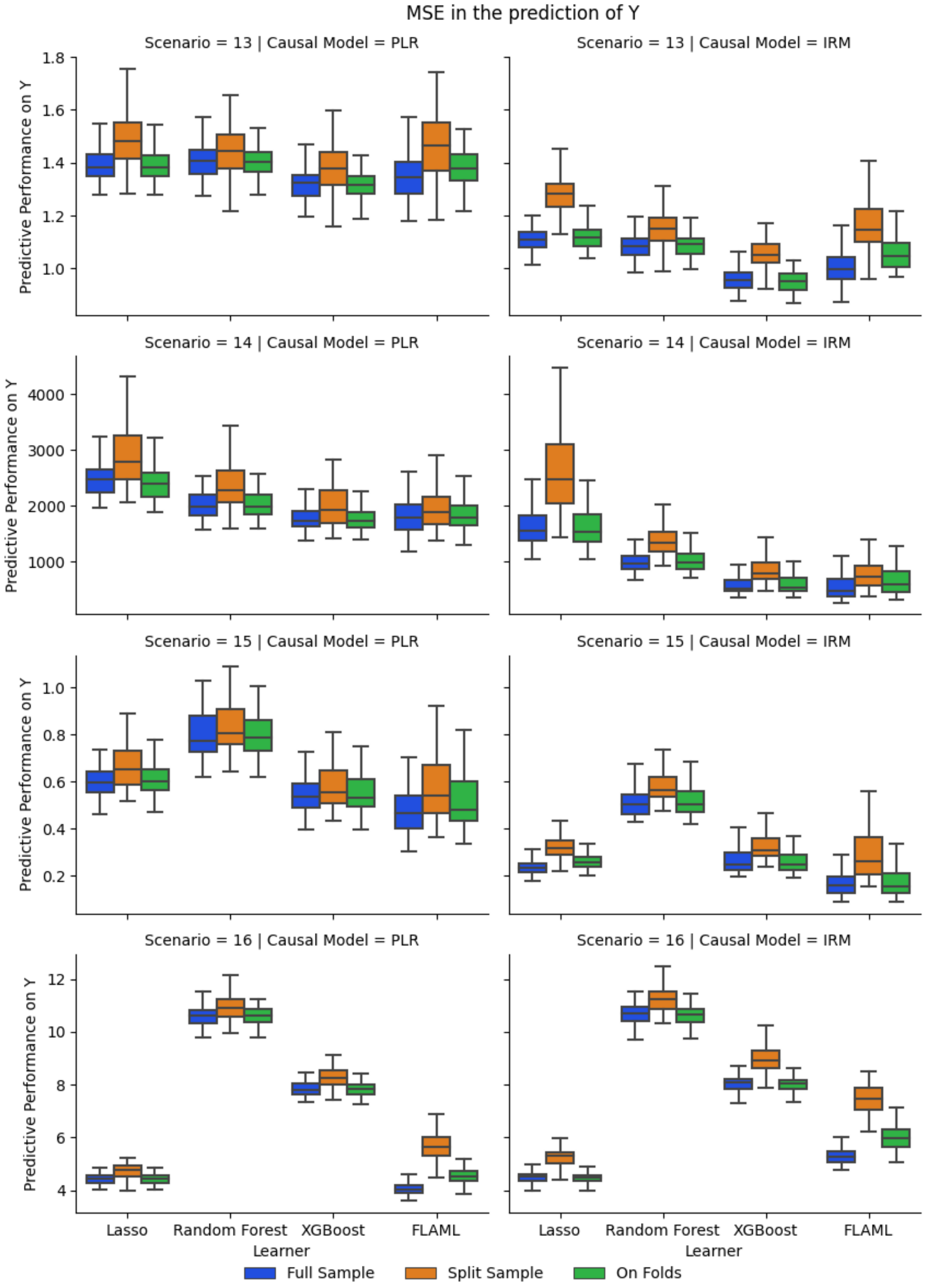

Figure 22: Predictive Performance on Y of ACIC DGP 13-15

E.4. Combined Loss

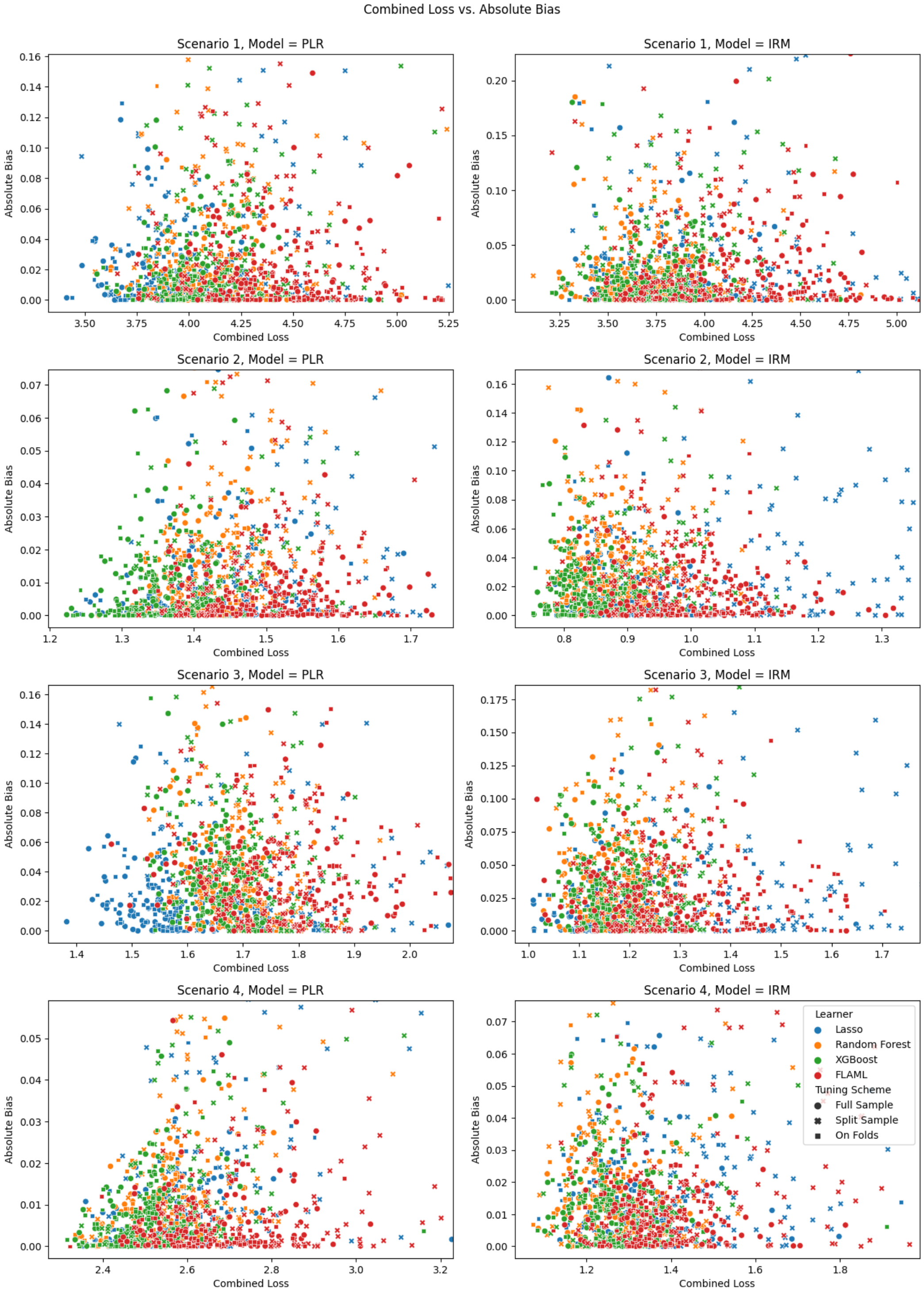

Figure 23: Combined Loss of ACIC DGP 1-4

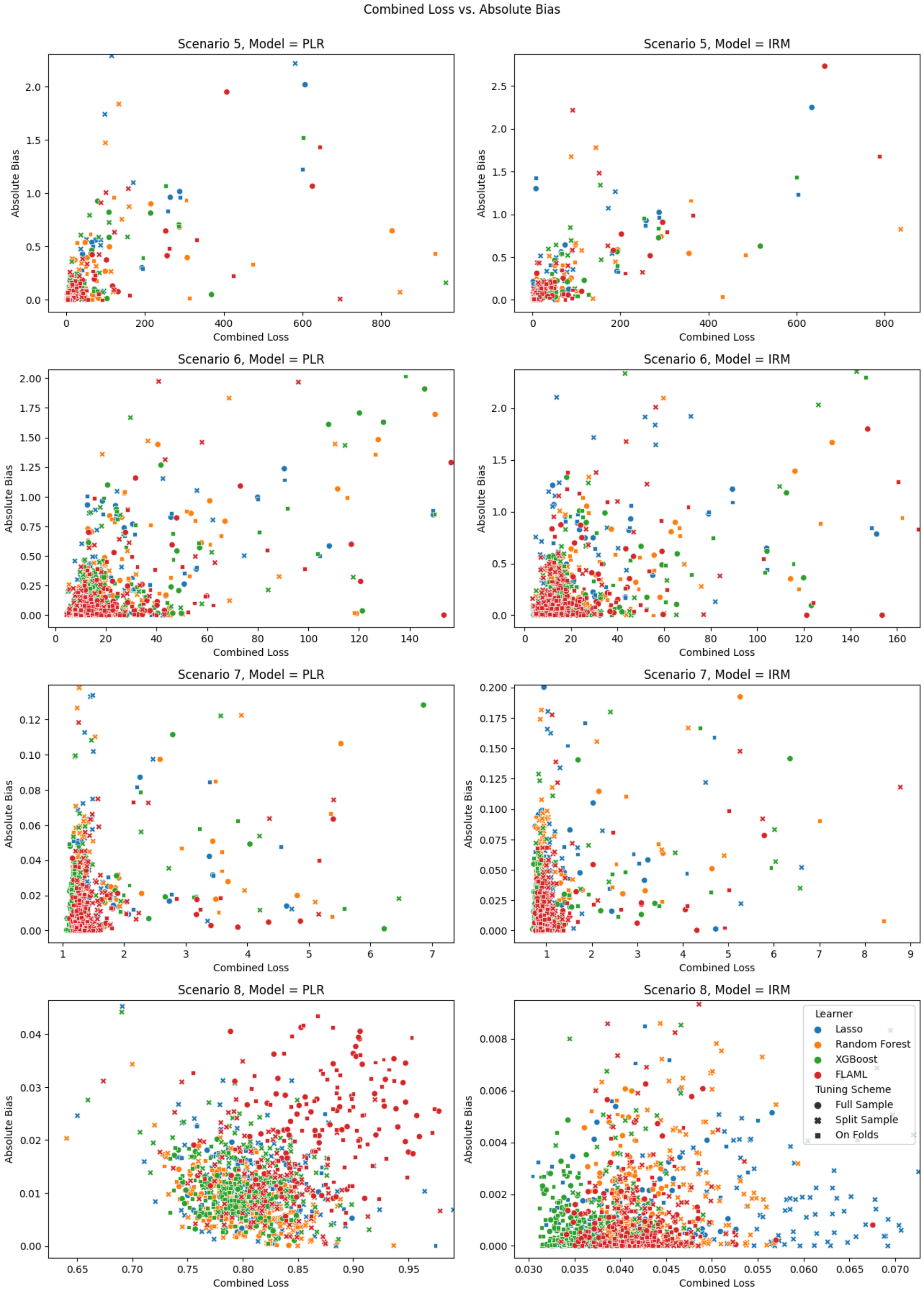

Figure 24: Combined Loss of ACIC DGP 5-8

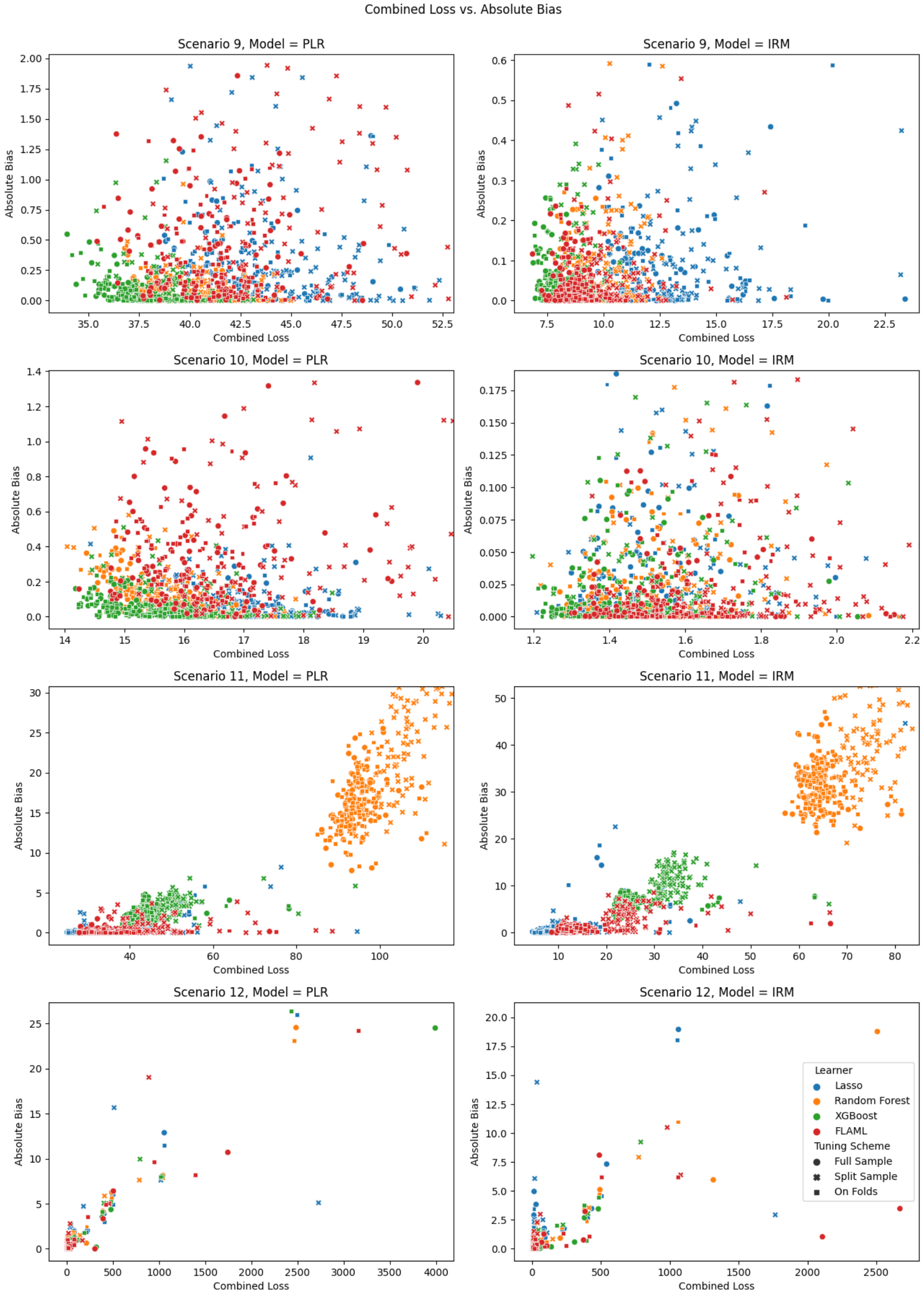

Figure 25: Combined Loss of ACIC DGP 9-12

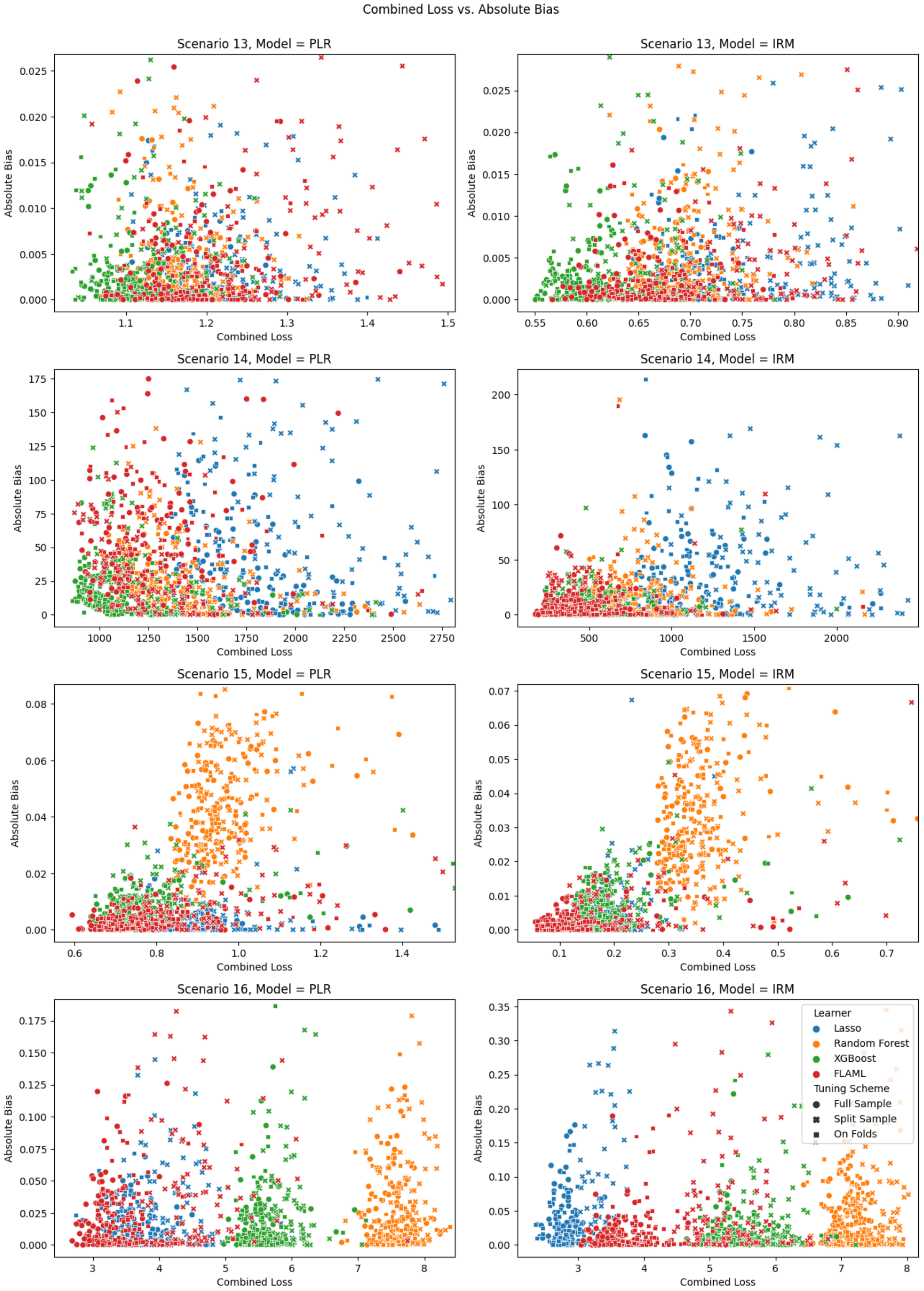

Figure 26: Combined Loss of ACIC DGP 13-15

E.5. RRMSE-1 vs. Bias vs. Combined Loss PLR

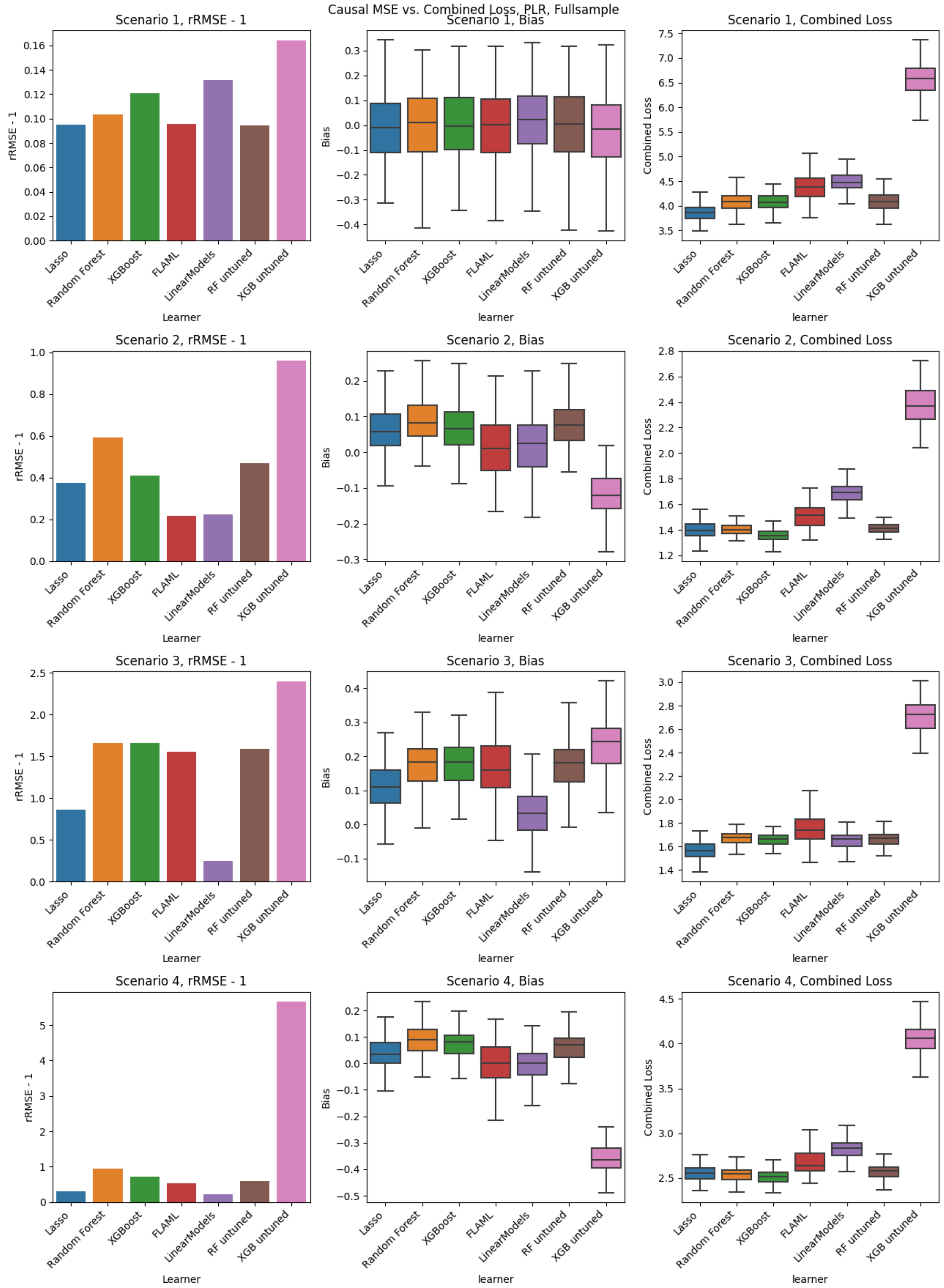

Figure 27: Combined Loss of ACIC DGP 1-4

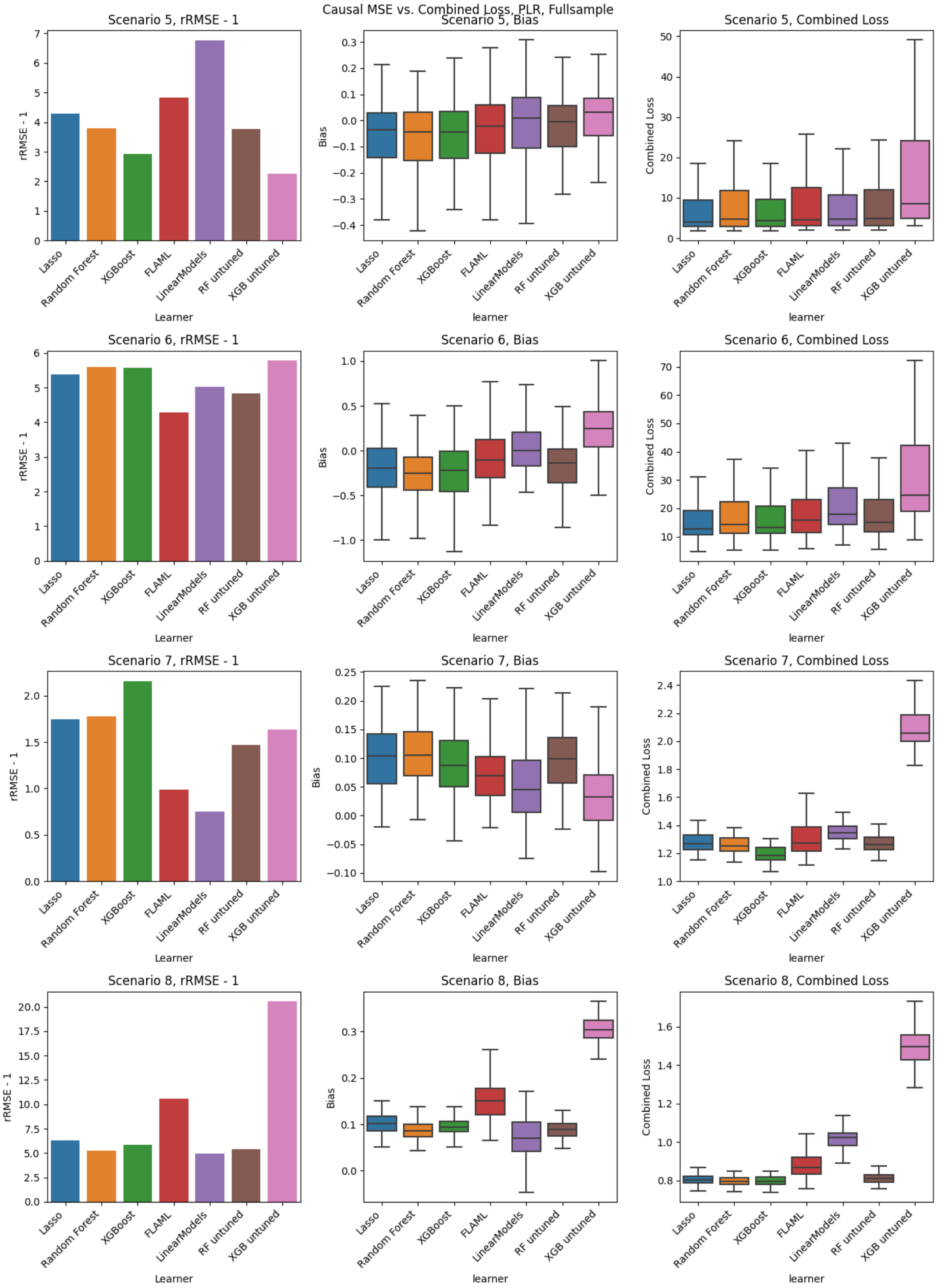

Figure 28: Combined Loss of ACIC DGP 5-8

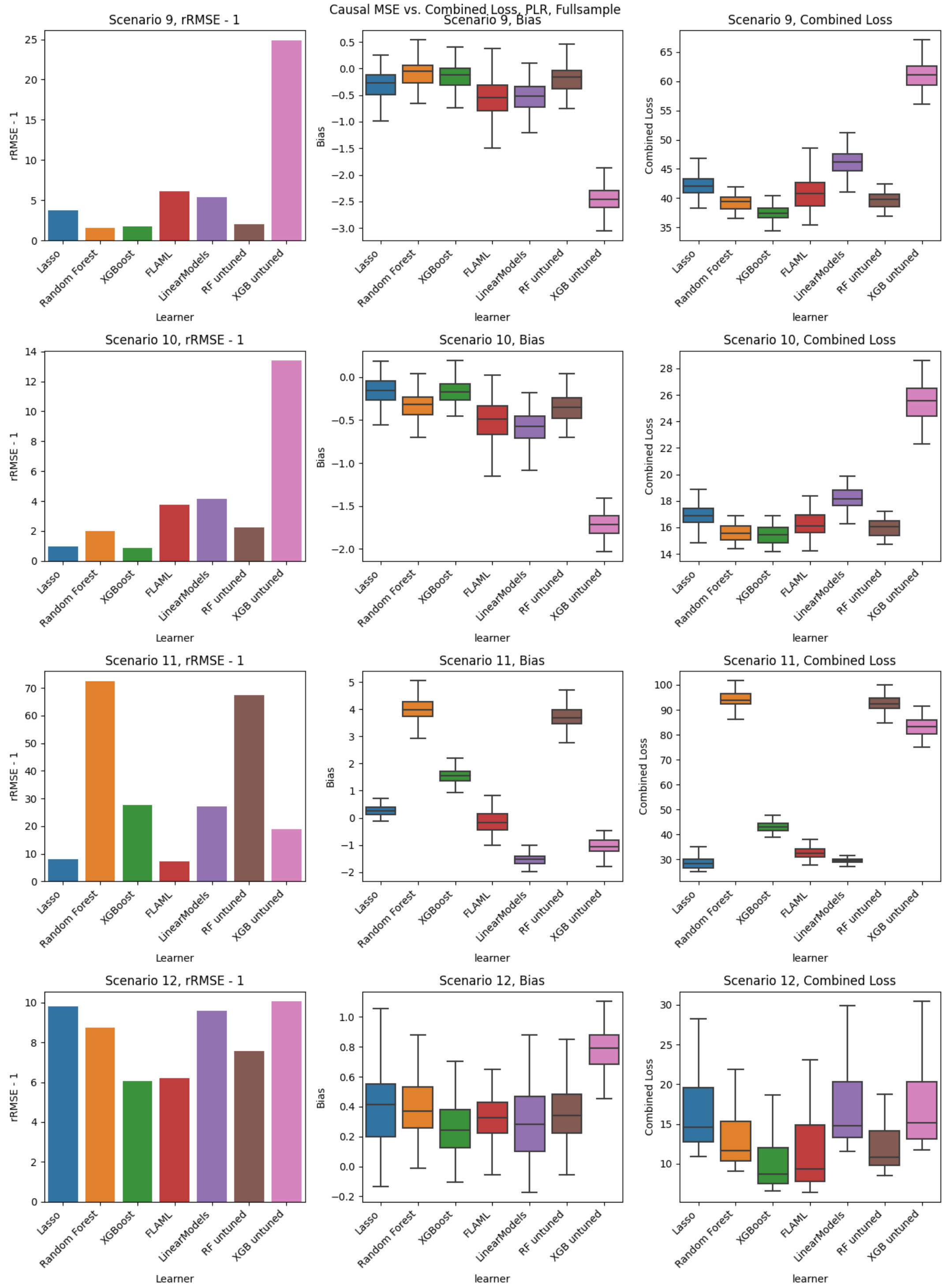

Figure 29: Combined Loss of ACIC DGP 9-12

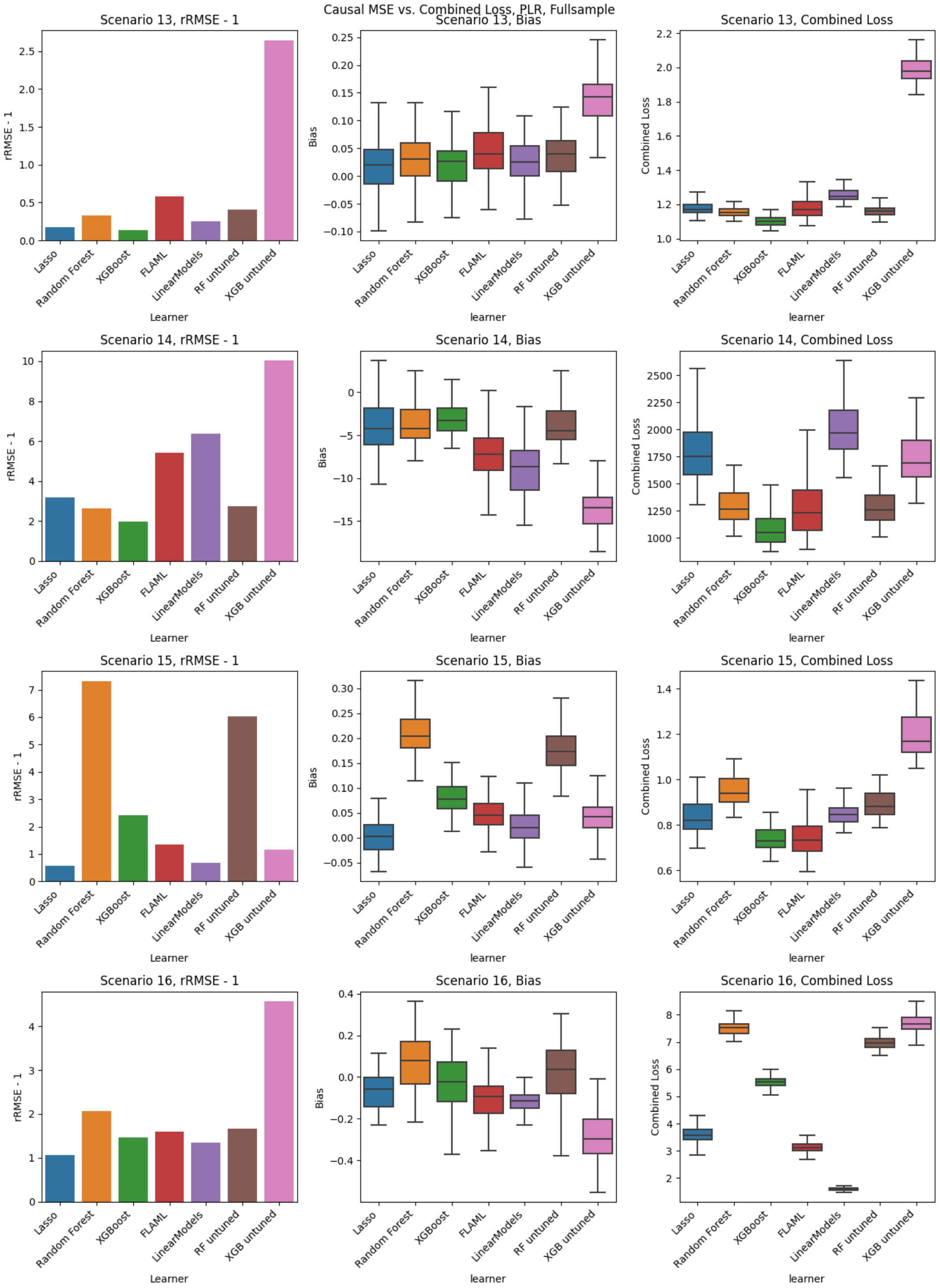

Figure 30: Combined Loss of ACIC DGP 13-15

E.6. RRMSE-1 vs. Bias vs. Combined Loss IRM

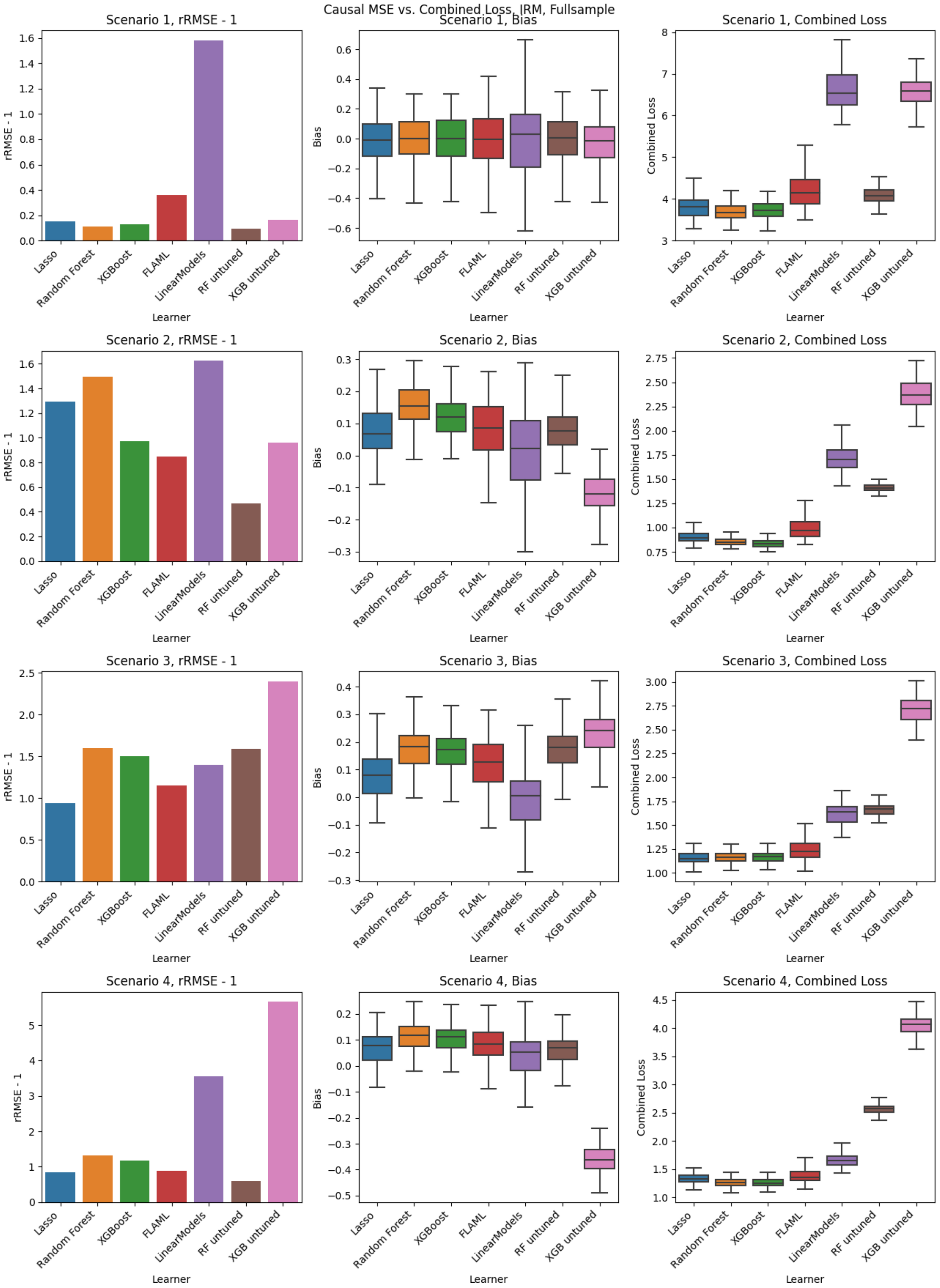

Figure 31: Comparison of RRMSE-1, Bias and Combined loss of ACIC DGP 1-4

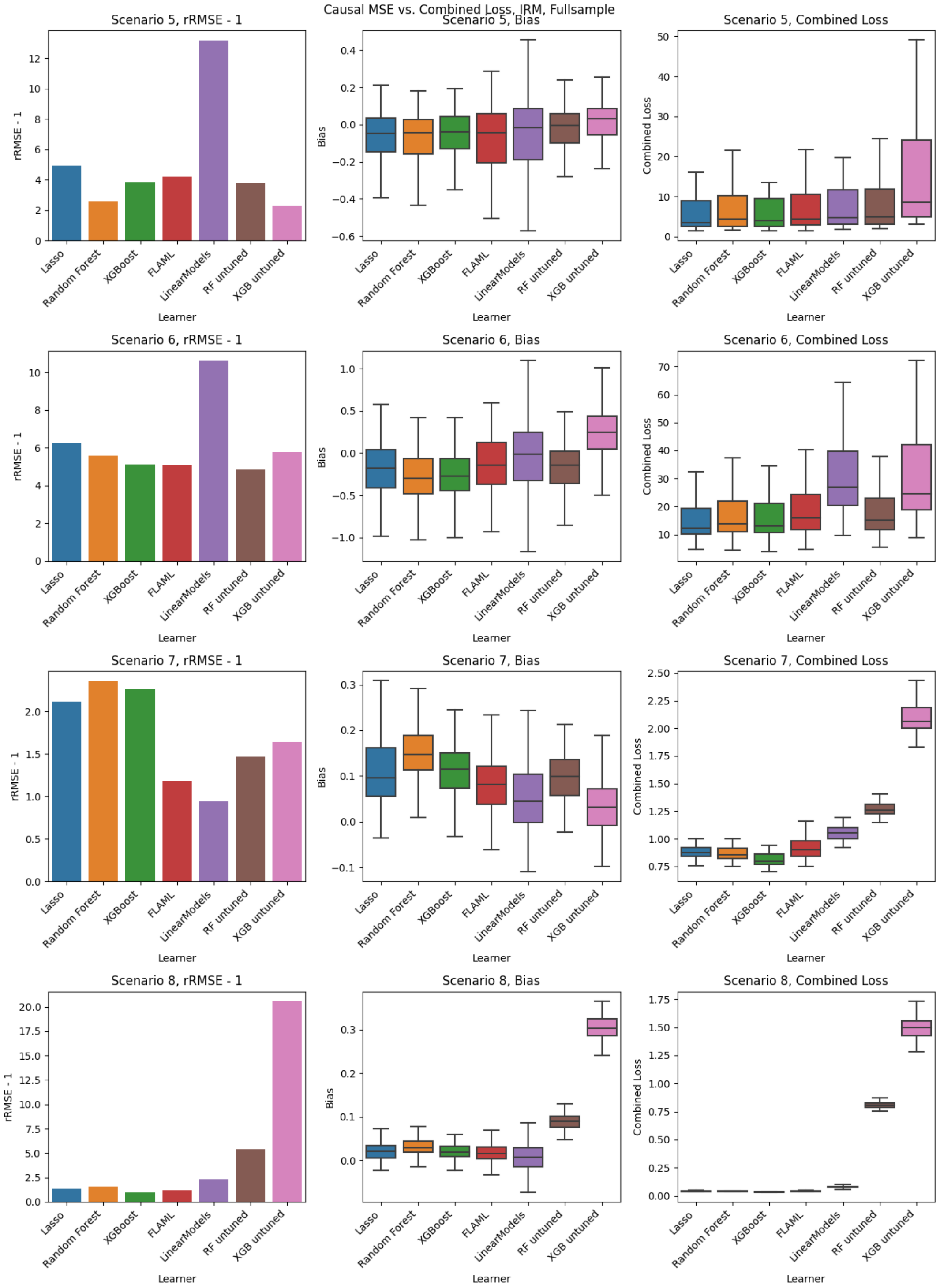

Figure 32: Comparison of RRMSE-1, Bias and Combined loss of ACIC DGP 5-8

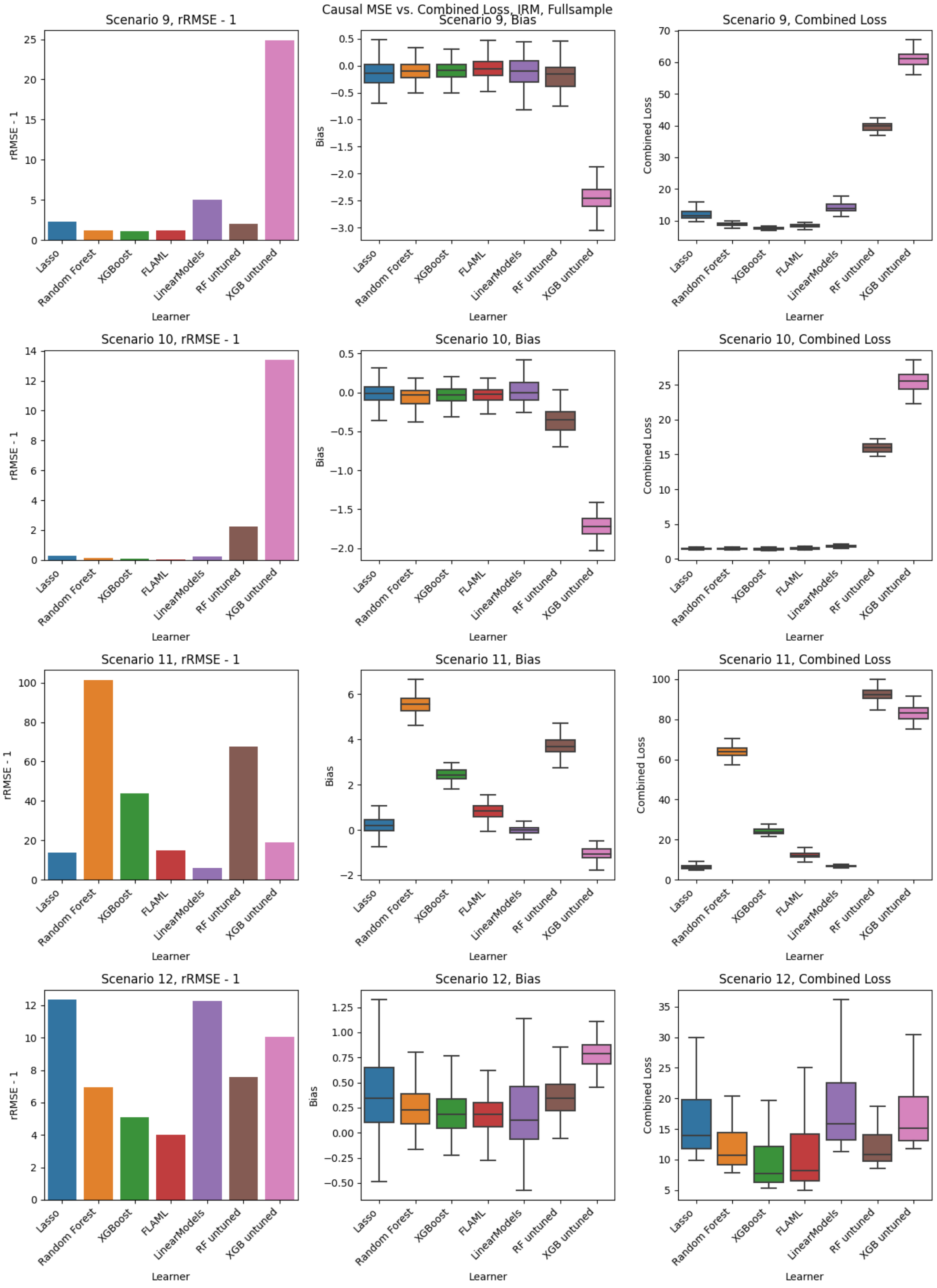

Figure 33: Comparison of RRMSE-1, Bias and Combined loss of ACIC DGP 9-12

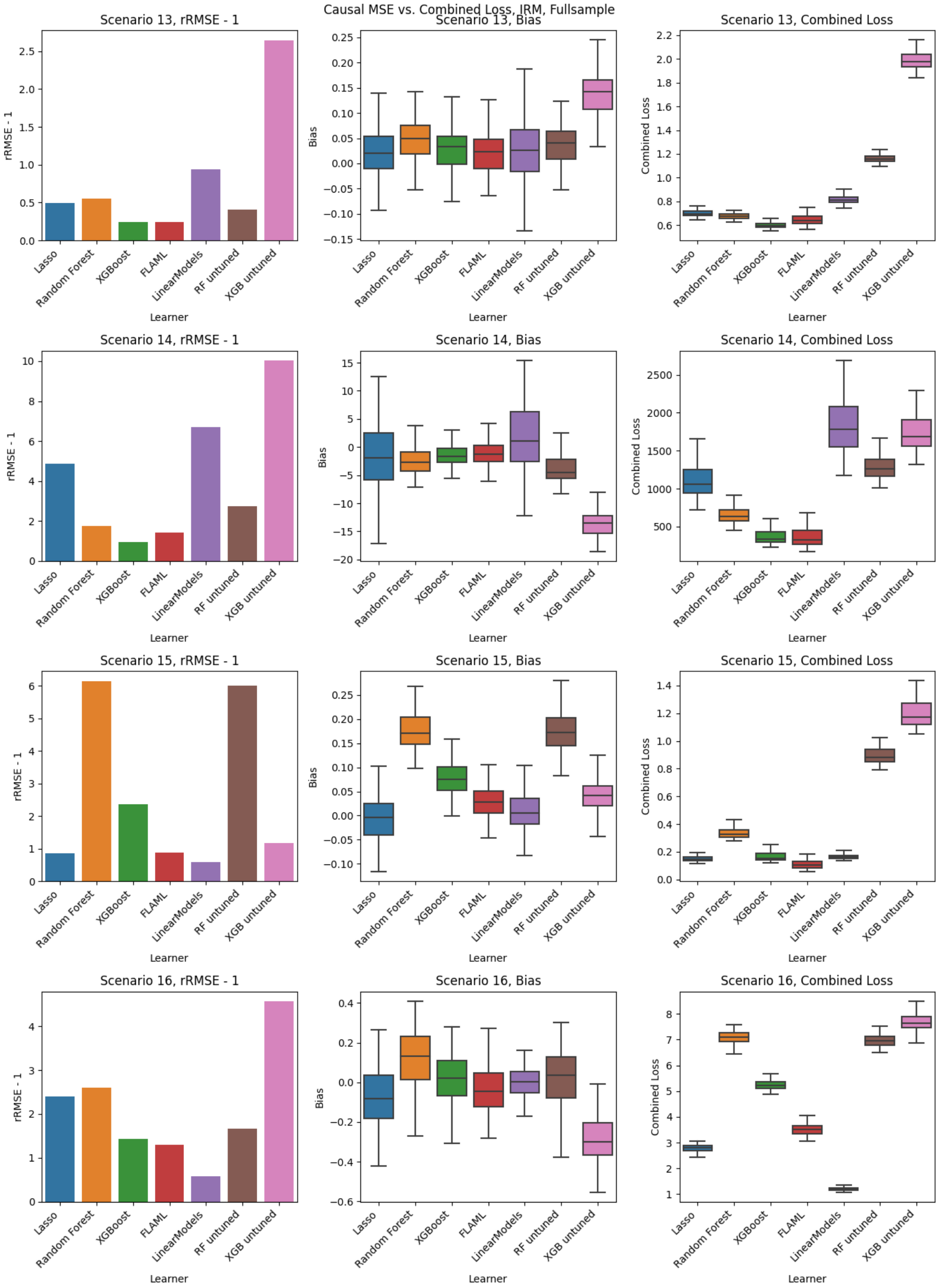

Figure 34: Comparison of RRMSE-1, Bias and Combined loss of ACIC DGP 13-15

Appendix F. ACIC 2019 DGP overview

In the following, we present a rough structure of the DGPs used. This is meant for an understanding of how the DGP look, presenting the exact data generating process with all coefficients would be infeasible. The X_i are drawn from multiple distributions in multiple copula.

F.1. DGP 1

$$\begin{aligned}
p &= \alpha_0 + \sum_{j=1}^{200} \alpha_j * X_j \\
A &\sim Bin(1, \text{sig}(p)) \\
Y &= \theta * A + \sum_{i=1}^{200} \beta_i * X_i + \epsilon \\
\epsilon &\sim \mathcal{N}(0, 2))
\end{aligned}$$

F.2. DGP 2

$$\begin{aligned}
p &= \alpha_0 + \alpha_1 * \sqrt{X_1} + \alpha_2 * X_5 + \alpha_3 * X_{32} + \alpha_4 X_5 * X_{32} + \alpha_5 * X_{70} \\
&\quad + \alpha_6 * X_{70}^2 + \alpha_7 * [\mathbb{1}[X_{101} > 2.5]] + \alpha_8 * X_{150} + \alpha_9 * [\mathbb{1}[X_{179} < -0.5]] * (X_{179} + 1.5) \\
A &\sim Bin(1, \text{sig}(p)) \\
Y &= \theta * A + \beta_1 * \sqrt{X_1} + \beta_2 * X_5 + \beta_3 * X_{23} + \beta_4 * X_{32} + \beta_5 * X_5 * X_{32} + \beta_6 * X_{70} + \beta_7 * X_{70}^2 \\
&\quad + \beta_8 * [\mathbb{1}[X_{101} > 2.5]] + \beta_9 * X_{15} * X_{10} * [\mathbb{1}[X_{179} < -0.5]] * (X_{179} + 1.5) + \beta_{11} * X_{179} + \epsilon \\
\epsilon &\sim \mathcal{N}(0, 1)
\end{aligned}$$

F.3. DGP 3

$$\begin{aligned}
p &= \sum_{i=1}^{90} \alpha_i * X_i \quad \text{i are 90 random indices} \\
A &\sim Bin(1, \text{sig}(p)) \\
Y &= \sum_{i=1}^{90} \alpha_i * X_i \\
\epsilon &\sim \mathcal{N}(0, 1)
\end{aligned}$$

F.4. DGP 4

$$
\begin{aligned}
p = {} & \alpha_0 + \alpha_1 * X_2 + \alpha_2 * X_5 + \alpha_3 * X_2 * X_5 + \alpha_4 * X_{12} + \alpha_5 * X_{23} \\
& + \alpha_6 * X_{23}^2 + \alpha_7 * X_{12} * X_{23}^2 + \alpha_8 * \sqrt{X_{67}} + \alpha_9 * X_{77} + \alpha_{10} * [\mathbb{1}[X_{89} > 19]] \\
& + \alpha_{11} * [\mathbb{1}[X_{95} > 5]] * (X_{95} - 3) + \alpha_{12} * \exp(X_{106}) + \alpha_{13} * X_{122} + \alpha_{14} * X_{146} + \alpha_{15} * X_{122} * X_{146} \\
& + \alpha_{16} * X_{150} + \alpha_{17} * X_{168} + \alpha_{18} * [\mathbb{1}[X_{199} > 1]] \\
A \sim {} & Bin(1, \mathrm{sig}(p)) \\
Y = {} & (\theta * A) + \beta_1 + \beta_2 * X_2 + \beta_3 * X_5 + \beta_4 * X_2 * X_5 + \beta_5 * X_{12} \\
& + \beta_6 * X_{23} + \beta_7 * X_{23}^2 + \beta_8 * X_{12} * X_{23}^2 + \beta_9 * X_{40} + \beta_{10} * \sqrt{X_{67}} + \beta_{11} * X_{77} \\
& + \beta_{12} * [\mathbb{1}[X_{89} > 19]] + \beta_{13} * [\mathbb{1}[X_{95} > 5]] * (X_{95} - 3) + \beta_{14} * \exp(X_{106}) + \beta_{15} * X_{122} + \beta_{16} * X_{133} \\
& + \beta_{17} * X_{146} + \beta_{18} * X_{122} * X_{146} + \beta_{19} * X_{150} * \beta_{20} * X_{168} + \beta_{21} * X_{198} \\
& + \beta_{22} * [\mathbb{1}[X_{199} > 1]] + \epsilon \\
\epsilon \sim {} & t(5)
\end{aligned}
$$

F.5. DGP 5

$$
\begin{aligned}
P = {} & \alpha_0 + \alpha_1 * X_{23} + \alpha_2 * X_{23}^2 + \alpha_3 * \sqrt{X_{67}} + \alpha_4 * X_{77} \\
& + \alpha_5 * [\mathbb{1}[X_{89} > 19]] + \alpha_6 * [\mathbb{1}[X_{95} > 5]] * (X_{95} - 3) + \alpha_7 * \exp(X_{106}) + \alpha_8 * X_{122} \\
& + \alpha_9 * X_{146} + \alpha_{10} * X_{122} * X_{146} + \alpha_{11} * X_{150} + \alpha_{12} * X_{168} + \alpha_{13} * [\mathbb{1}[X_{199} > 1]] \\
A \sim {} & Bin(1, \mathrm{sig}(p)) \\
Y = {} & \exp(\theta * A + \beta_1 + \beta_2 * \sqrt{X_{67}} + \beta_3 * X_{77} + \beta_4 * [\mathbb{1}[X_{89} > 19]] \\
& + \beta_5 * \ \mathbb{1}[X_{95} > 5]] * (X_{95} - 3) + \beta_6 * \exp(X_{106}) + \beta_7 * X_{122} + \beta_8 * X_{146} + \beta_9 * X_{146} * X_{122} \\
& + \beta_{10} * X_{150} + \beta_{11} * X_{168} + \beta_{12} * [\mathbb{1}[X_{199} > 1]] + \epsilon) \\
\epsilon \sim {} & t(12)
\end{aligned}
$$

F.6. DGP 6

$$
\begin{aligned}
p = {} & \alpha_0 + \alpha_1 * X_4 + \alpha_2 * X_{19} + \alpha_3 * X_{44} \\
A \sim {} & Bin(1, \mathrm{sig}(p)) \\
Y = {} & \exp(A * (\theta + \tau * X_{55}) + \beta_1 + \beta_2 * X_4 + \beta_3 * X_{19} + \beta_4 * X_{44} + \epsilon) \\
\epsilon \sim {} & t(19), \theta = 0.4, \tau = 0.2
\end{aligned}
$$

F.7. DGP 7

$$
\begin{aligned}
p &= \alpha_0 + \alpha_1 * X_3 + \alpha_2 * X_6 + \alpha_3 * X_3 * X_6 + \alpha_4 * X_{24} + \alpha_5 * X_{24}^2 + \alpha_6 * X_{35} + \alpha_7 * X_{68} \\
&\quad + \alpha_8 * \sqrt{X_{68}} + \alpha_9 * X_{35} * \sqrt{X_{68}} + \alpha_{10} * [\mathbb{1}[X_{96} < 2]] * (X_{96} - 1) + \alpha_{11} * \exp{(X_{107})} + \alpha_{12} * X_{123} \\
&\quad + \alpha_{13} * X_{149} + \alpha_{14} * X_{123} * X_{149} + \alpha_{15} * X_{151} + \alpha_{16} * 1/X_{169} + \alpha_{17} * X_{200} \\
A &\sim Bin(1, \mathrm{sig}(p)) \\
Y &= \theta * A + \beta_1 + \beta_2 * X_3 + \beta_3 * X_6 + \beta_4 * X_3 * X_6 + \beta_5 * X_{24} + \beta_6 * X_{24}^2 \\
&\quad + \beta_7 * X_{35} + \beta_8 * X_{40} + \beta_9 * X_{68} + \beta_{10} * \sqrt{X_{68}} + \beta_{11} * X_{35} * \sqrt{X_{68}} \\
&\quad + \beta_{12} * [\mathbb{1}[X_{96} < 2]] * (X_{96} - 1) + \beta_{13} * \exp X_{107} + \beta_{14} * X_{123} + \beta_{15} * X_{133} + \beta_{16} * X_{149} \\
&\quad + \beta_{17} * X_{123} * X_{149} + \beta_{18} * X_{151} + \beta_{19} * 1/X_{169} + \beta_{20} * X_{198} + \beta_{21} * X_{200} + \epsilon \\
\epsilon &\sim \mathcal{N}(0, 1)
\end{aligned}
$$

F.8. DGP 8

$$
\begin{aligned}
p &= \alpha_0 + \alpha_1 * \log(X_7 + 1) + \alpha_2 * 1/X_{16} + \alpha_3 * |X_{51}| + \alpha_4 * X_{156} \\
&\quad + \alpha_5 * X_{156}/\log(X_7 + 0.5) + \alpha_6 * X_{163}^2 \\
A &\sim Bin(1, \mathrm{sig}(p)) \\
\overline{y} &= \theta * A + \beta_1 + \beta_2 * X_7 + \beta_3 * X_{16} + \beta_4 * X_{51} + \beta_5 * X_{156} \\
Y &= 10/(2 + \exp(-1 * \overline{y})) + \epsilon \\
\epsilon &\sim \mathcal{N}(0, 0.2)
\end{aligned}
$$

F.9. DGP 9

$$
\begin{aligned}
p &= \alpha_0 + \alpha_1 * \log(X_8) + \alpha_2 * 1/\sqrt{X_{17}} + \alpha_3 * \exp(-X_{52}) + \alpha_4 * |X_{157}| \\
&\quad + \alpha_5 * X_{157} * \log(X_8) + \alpha_6 * X_{164} + \alpha_7 * X_{165} + \alpha_8 * X_{164} * X_{165} \\
A &\sim Bin(1, \mathrm{sig}(p)) \\
\overline{y_1} &= \theta * A + \beta_1 + \beta_2 * X_8 + \beta_3 * X_{17} \\
\overline{y_2} &= \beta_4 * X_{52} + \beta_5 * X_{157} + \beta_6 * X_{166} \\
\tilde{y} &= \exp(\overline{y_1}) + (\overline{y_2} + 59) * (\overline{y_2} > -59.5) \\
Y &= \tilde{y} + \epsilon \\
\epsilon &\sim \mathcal{N}(0, 3)
\end{aligned}
$$

F.10. DGP 10

$$
\begin{aligned}
p &= \alpha_0 + \alpha_1 * X_1 + \alpha_2 * \log(X_8) + \alpha_3 * 1/\sqrt{X_{17}} + \alpha_4 * \exp(-X_{52}) + \alpha_5 * |X_{157}| \\
&\quad + \alpha_6 * X_{157} * \log(X_8) + \alpha_7 * X_{164} + \alpha_8 * X_{165} + \alpha_9 * |X_{157}| * X_{165} \\
A &\sim Bin(1, \text{sig}(p)) \\
Y &= A * (\theta + X_8 * \lambda + X_{157} * X_{166} * \delta) + \beta_1 + \beta_2 * X_8 + \beta_3 * X_{17} + \beta_4 * X_{52} \\
&\quad + \beta_5 * X_{157} + \beta_6 * X_{166} + \beta_7 * X_{157} * X_{166} + \epsilon \\
\epsilon &\sim t(4), \theta = 5, \lambda = 5, \delta = 0.5
\end{aligned}
$$

F.11. DGP 11

$$
\begin{aligned}
p &= \sum_{i=1}^{18} \alpha_i * X_i \quad \text{(18 random drawn indices)} \\
A &\sim Bin(1, \text{sig}(p)) \\
\tilde{Y} &= \sum_{i=1}^{23} \alpha_i * X_i + \theta * A \\
Y &= \tilde{Y}^2 + \epsilon \\
\epsilon &\sim N(0, 2)
\end{aligned}
$$

F.12. DGP 12

$$
\begin{aligned}
p &= \alpha_0 + \alpha_1 * (X_5 - 200) * (X_5 > 204) + \alpha_2 * \log(X_7 + 1) + \alpha_3 * 1/(X_{16}) + \alpha_4 * \sqrt{X_{25}} \\
&\quad + \alpha_5 * |X_{51}| + \alpha_6 * X_{96} + \alpha_7 * X_{96}/(\log(X_7 + 1) + 0.5) + \alpha_8 * X_{156} + \alpha_9 * X_{163}^2 \\
A &\sim Bin(1, \text{sig}(p)) \\
\overline{y} &= -0.5 * A + \beta_1 + \beta_2 * (X_5 - 200) * (X_5 > 204) + \beta_3 * \sqrt{X_{25}} + \beta_4 * X_{96} \\
&\quad + \beta_5 * X_{163}^2 + \beta_6 * |X_{169}| + \beta_7 * X_{188}^3 \\
Y &= 3/(\exp(-0.6 * \overline{y})) + \epsilon \\
\epsilon &\sim \mathcal{N}(0, 2)
\end{aligned}
$$

F.13. DGP 13

$$
\begin{aligned}
p &= \alpha_0 + \alpha_1 * (X_5 - 200) * (X_5 > 204) + \alpha_2 * \sqrt{X_{25}} + \alpha_3 * (X_5 - 200) * (X_5 > 204) * \sqrt{X_{25}} \\
&\quad + \alpha_4 * X_{96} + \alpha_5 * X_{163} + \alpha_6 * X_{96} * X_{163} + \alpha_7 * X_{163}^2 + \alpha_8 * |X_{169}| + \alpha_9 * X_{188}^3 \\
&\quad + \alpha_{10} * |X_{169}| * X_{188}^3 \\
A &\sim Bin(1, \mathrm{sig}(p)) \\
\tilde{y} &= A * (-0.5 - 0.25 * X_{163}^2) + \beta_1 + \beta_2 * (X_5 - 200) * (X_5 > 204) + \beta_3 * \log(X_7 + 1) \\
&\quad + \beta_4 * 1/X_{16} + \beta_5 * |X_{51}| + \beta_6 * X_{96} + \beta_7 * X_{96}/(\log(X_7 + 1) + 0.5) + \beta_8 * X_{156} \\
&\quad + \beta_9 * X_{163}^2 + \beta_{10} * X_{188}^2 \\
Y &= \tilde{y} + \epsilon \\
\epsilon &= (1 - A) * \epsilon_1 + A * \epsilon_2 \\
\epsilon_1 &\sim \mathcal{N}(0, 1) \\
\epsilon_2 &\sim \mathcal{N}(0, 0.5)
\end{aligned}
$$

F.14. DGP 14

$$
\begin{aligned}
p &= \alpha_0 + \alpha_1 * \log(X_8) + \alpha_2 * 1/\sqrt{X_{17}} + \alpha_3 * \exp(X_{52}) + \alpha_4 * X_{100} + \alpha_5 * |X_{157}| \\
&\quad + \alpha_6 * |X_{157}| * \log(X_8) + \alpha_7 * X_{162}^2 + \alpha_8 * X_{165} + \alpha_9 * X_{100} * X_{165} \\
\overline{y_1} &= 0.75 * A + \beta_1 + \beta_2 * \log(X_8) + \beta_3 * \sqrt{X_{17}} + \beta_4 * X_{52} + \beta_5 * |X_{157}| \\
\overline{y_2} &= 10 * A + |\beta_6 * X_{162} + \beta_7 * X_{166} + \beta_8 * (X_{188}^2) * (X_{188} > 0.4)| \\
Y &= \exp(\overline{y_1}) + \overline{y_2} + \epsilon \\
\epsilon &\sim \mathcal{N}(0, 4)
\end{aligned}
$$

F.15. DGP 15

$$\begin{aligned}
p &= \alpha_0 + \alpha_1 * (X_{10} - 5) * (X_{10} > 5) + \alpha_2 * \sqrt{X_{25}} + \alpha_3 * (X_{10} - 5) * (X_{10} > 5) * \sqrt{X_{25}} \\
&\quad + \alpha_4 * X_{42} + \alpha_5 * \log(X_{52}) + \alpha_6 * |X_{70}|^{1/3} + \alpha_7 * X_{96} \\
&\quad + \alpha_8 * \log(X_{52}) * X_{96} + \alpha_9 * X_{158} + \alpha_{10} * X_{96} * X_{158} \\
&\quad + \alpha_{11} * X_{163}^2 + \alpha_{12} * |X_{169}| + \alpha_{13} * X_{188}^3 + \alpha_{14} * X_{192} + \alpha_{15} * X_{188}^3 * X_{192} \\
A &\sim Bin(1, \text{sig}(p)) \\
Y &= A * (-0.75 - 0.25 * X_{192} + 0.6 * X_{51}) + \beta_1 + \beta_2 * \log(X_7 + 1) + \beta_3 * (1/X_{16}) + \beta_4 * \sqrt{X_{25}} \\
&\quad + \beta_5 * \log(X_{52}) + \beta_6 * X_{96} + \beta_7 * X_{96}/((\log(X_7 + 1) + 0.5) \\
&\quad + \beta_8 * X_{158} + \beta_9 * X_{163}^2 + \beta_{10} * X_{188}^2 + \beta_{11} * X_{192} + \beta_{12} * X_{96} \\
&\quad + \beta_{13} * X_{188}^3 * X_{192} + \epsilon \\
\epsilon &= (1 - A) * \epsilon_1 + A * \epsilon_2 \\
\epsilon_1 &\sim \mathcal{N}(0, 0.05) \\
\epsilon_2 &\sim \mathcal{N}(0, 0.1)
\end{aligned}$$

F.16. DGP 16

$$\begin{aligned}
p &= \alpha_0 + \sum_{j=1}^{200} \alpha_j * X_j] \\
A &\sim Bin(1, \text{sig}(p)) \\
Y &= (\theta * A) + \sum_{i=1}^{200} \beta_i * X_i + \epsilon \\
\epsilon &\sim t(8)
\end{aligned}$$